Final Report on the Scientific and Engineering Design of a SOFT X-RAY DIODE ARRAY DIAGNOSTIC SYSTEM FOR JET (KJ 1)

JET Contract Number JBO/9010

H.U. Fahrbach, H. Goss,
E. Harmeyer, G. Schramm

IPP 1/209 July 1982
Reprint of IPP-JET-Report No. 6

MAX-PLANCK-INSTITUT FÜR PLASMAPHYSIK

8046 GARCHING BEI MÜNCHEN

MAX-PLANCK-INSTITUT FÜR PLASMAPHYSIK

GARCHING BEI MÜNCHEN

Final Report on the Scientific and Engineering Design of a SOFT X-RAY DIODE ARRAY DIAGNOSTIC SYSTEM FOR JET (KJ 1)

JET Contract Number JBO/9010

H.U. Fahrbach, H. Goss,
E. Harmeyer, G. Schramm

IPP 1/209 July 1982
Reprint of IPP-JET-Report No. 6

Die nachstehende Arbeit wurde im Rahmen des Vertrages zwischen dem Max-Planck-Institut für Plasmaphysik und der Europäischen Atomgemeinschaft über die Zusammenarbeit auf dem Gebiete der Plasmaphysik durchgeführt.

Abstract

This report describes the Soft-X-Ray Diode Array Diagnostic System for JET. It was designed by the IPP under an Article 14 contract for Phase I. The diagnostics will be capable of measuring the Soft-X-Ray emission from H and D plasmas in JET with high resolution in space and time. Two slot-hole cameras with 150 detectors viewing the same toroidal cross-section of the plasma are foreseen. Thin beryllium and aluminium filters in the line of sight of the detectors allow simultaneous measurements within different limits of the X-ray spectrum. Heavy shielding against neutron and gamma radiation is provided in order to reduce radiation induced signals and to increase detector lifetimes. The signals of 100 detectors can be simultaneously sampled with a sampling rate variable up to 250 KHZ and stored in 12 bit memories of about 20 Kwords size.

1. Introduction

This report presents the design of the Soft X-Ray Diode Array Diagnostic System for JET. The proposal was worked out by the IPP at Garching in a Phase I contract and includes the completion of the scientific and engineering design of the diagnostics to the point, where an immediate start can be made on Phase II.

This edition is a reprint of the IPP-JET-Report No. 6. The curves in figures 2 and 13 have been modified because of errors in the original calculations. The conclusions remain unaffected by the new results.

1.1 Scientific Objectives

Three major aims of the soft X-ray diode array measurements in JET have been formulated:

- to measure fluctuations in the emission in order to study the mode structure of MHD oscillations and locate rational q-surfaces;
- to measure the radial profile of the absolute intensity of the emission in the soft X-ray region of the spectrum;
- to measure the coarse spectrum of the soft X-ray emission by means of filters.

The most important task of this diagnostics is to provide a means of investigating MHD and other fluctuations and disruptive instabilities in JET. But the additional capabilities of this system are no less valuable. A large portion of energy lost by radiation from the central region of a high-temperature plasma belongs to the ultra-soft and soft X-ray regions of the spectrum. Absolute measurement of the emission of radiation in this spectral range is thus very useful for energy balance considerations of JET plasmas and will supplement bolometric measurements also because of the high resolution in time and space which can be obtained with the X-ray diode system.

As impurity radiation (line radiation and continuum radiation) normally exceeds hydrogen radiation in typical tokamak discharges, quantitative analysis of soft X-ray radiation will help to study the distributions of impurities, identify impurity transport

phenomena and thus facilitate optimization of plasma conditions.

Application of different spectral filters, finally, will give a rough insight into the type of impurities involved and thus contribute to the improvement of plasma parameters. Moreover, rough electron temperature measurements may be performed by the filter method. They can support other methods of electron temperature determination, particularly because these are not capable of reaching the inner half of the JET plasma. The high resolution in time and space may be used for detailed study of developments which take place within small regions, e.g. magnetic islands.

2. Principles and Performance of the Soft X-Ray Array

2.1 General Layout of the Diagnostics

The diagnostic system consists of two slot-hole X-ray imaging cameras which view the same toroidal cross-section of the plasma in Octant 2 of JET, the one vertically from above and the other horizontally from outside the torus (Fig. 1). Eighty detectors in the horizontal and fifty in the vertical camera measure the X-ray emission between photon energies of 0.3 and 15 keV from nearly the entire plasma cross-section. Five to ten additional detectors shielded against the soft X-rays by thin aluminium plates are distributed in each detector array to allow the subtraction of signals generated by neutron and gamma radiation.

The detectors are connected to the preamplifiers at the rear of the cameras by means of ~25 cm long cables with twisted pairs of wires. This length, unavoidable because of constraints in the mechanical design, is regarded as the maximum tolerable value for the desired bandwidth and the level of noise and pick-up.

The electronics and data-acquisition system outside the torus hall will be restricted to 100 channels in order to reduce the costs of the diagnostics. The attachment of electronic channels to de-

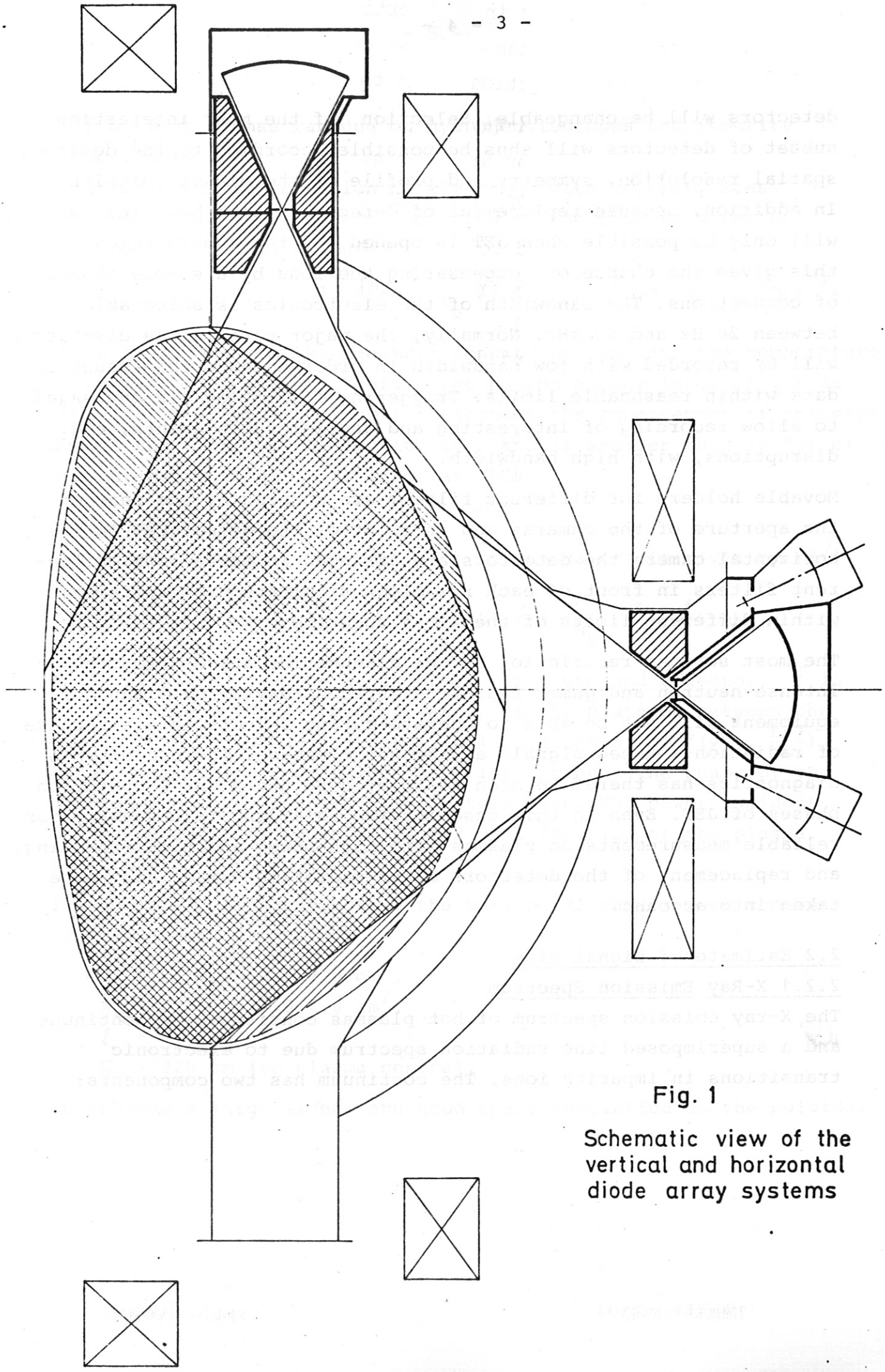

Fig. 1

Schematic view of the vertical and horizontal diode array systems

detectors will be changeable. Selection of the most interesting subset of detectors will thus be possible according to the desired spatial resolution, symmetry and profile of the plasma emission. In addition, because replacement of detectors which have failed will only be possible when JET is opened and the camera removed, this gives the chance of compensating the loss by a simple change of connections. The bandwidth of the electronics is selectable between 20 Hz and 50 kHz. Normally, the major part of the discharges will be recorded with low bandwidth in order to keep the amount of data within reasonable limits. Triggering facilities are envisaged to allow recording of interesting and unpredictable events, e.g. disruptions, with high bandwidth.

Movable holders for different filters are mounted at the rear of the aperture of the cameras and in front of the detectors. In the horizontal camera the detectors are arranged in three rows. Different filters in front of each row allow simultaneous measurements within different limits of the X-ray spectrum.

The most serious restriction of the diagnostics arises from the intense neutron and gamma radiation. Present-day X-ray diagnostic equipment will not be able to operate during D-T discharges because of radiation-induced signals and detector damage. The use of this diagnostics has therefore been restricted to the H and D operation phases of JET. Even in this case massive shielding is necessary for reliable measurements on plasmas with high-power additional heating, and replacement of the detectors after radiation damage has to be taken into account.

2.2 Estimate of Signal Size

2.2.1 X-Ray Emission Spectrum

The X-ray emission spectrum of hot plasmas consists of a continuum and a superimposed line radiation spectrum due to electronic transitions in impurity ions. The continuum has two components:

- free-free bremsstrahlung on hydrogen isotopes and impurity ions and
- free-bound recombination of electrons with impurity ions.

The power P in units of W/cm^2 emitted in the continuum can be described by the equation

$$(1) \qquad P = 5.35 \cdot 10^{-31} \cdot n_e^2 \cdot T_e^{1/2} \cdot \zeta \cdot \left(e^{-E_{min}/T_e} - e^{-E_{max}/T_e} \right) ,$$

where n_e and T_e are the electron density per cm^3 and the temperature in keV, and E_{min} and E_{max} define the photon energy interval ΔE in keV /1/. The factor ζ takes into account the enhancement of emission due to the presence of impurity ions and is smaller than 10 for clean discharges, but can be as large as 1000.

2.2.2 Imaging Geometry

The power measured by the detector in the camera is given by /2/:

$$(2) \qquad P_D(\Delta E) = \frac{A_A \cdot A_D}{4\pi \cdot \ell^2} \int_{L=L_0}^{L_1} P(\Delta E, L) \cdot f\left(\frac{A_A}{A_D}, \frac{L - \ell}{L}\right) dL ,$$

where A_A and A_D are the areas of the aperture and detector, ℓ is the distance between these two and L is the distance between the detector and volume of emission, all in units of cm. $f\left(\frac{A_A}{A_D}, \frac{L-\ell}{L}\right)$ is a correction factor which takes into account the shape of the viewing beam and is about 1.15 in this case. The power incident on the detector is shown in Fig. 2 as a function of the plasma temperature.

The geometrical parameters of the horizontal camera were chosen as follows:

$A_D = h_D \cdot \ell_D = 0.5 \cdot 2.0 \ cm^2$,
$A_A = h_A \cdot \ell_A = 1.0 \cdot 4.0 \ cm^2$,
$\ell = 70$ cm,
$L = 320$ cm (to plasma centre).

To achieve a large signal and good space resolution in the poloidal

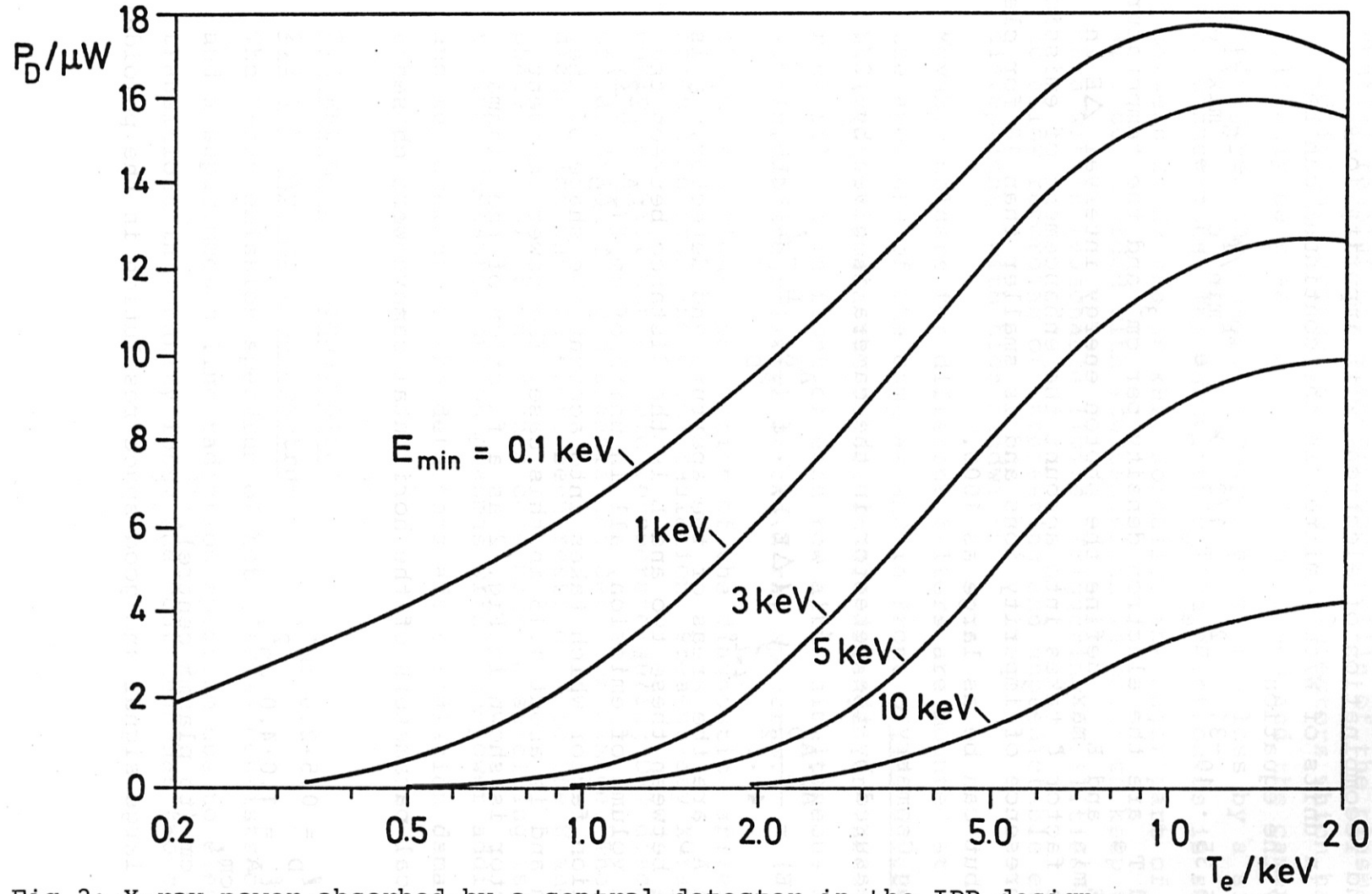

Fig.2: X-ray power absorbed by a central detector in the IPP design geometry as a function of the electron temperature for filters with different cut-off energy. The values refer to plasmas with flat temperature and density profiles, a radius of 1m, ζ = 1, $n_e = 3 \times 10^{13} cm^{-3}$. A volume emission of 1 mW/cm^3 leads to a power of 15 µW absorbed by the detector without filter and a signal current of 4.2 µA.

direction, the dimensions of the aperture and detector are 4 times smaller in the poloidal (h_A, h_D) than in the toroidal direction (ℓ_A, ℓ_D).
The space resolution perpendicular to the viewing direction (full width at half maximum of the viewing beam) near the tangential point of the flux surfaces is then

$$(3) \qquad \cdot \mathrm{FWHM} = \frac{L}{\ell} h_A = 4.6 \text{ cm}.$$

This value is close to the distance between neighbouring viewing chords. The parameters of the vertical camera are only slightly different because of the different geometry of the vertical port. The discussion can therefore be confined to the horizontal camera.

The signal current of Si diodes is proportional to the absorbed power. The responsivity is 0.28 A/W, corresponding to a value of 3.6 eV required to produce one electron hole pair. This value is well established by different investigations /3,4/ and can be used for absolute calibration as long as the photon energy is high enough that absorption in the dead layer in front of the depletion region is negligible. At high photon energies the response curve drops because the detector becomes transparent. The curve of a 0.3 mm thick PIN diode is shown in Fig. 3.

To estimate the detector signal range, an idealized example is calculated. The emitted power of a pure hydrogen plasma with $n_{eo} = 3 \cdot 10^{13}$ cm^{-3}, $T_{eo} = 5$ keV, $\zeta = 1$ is

$$P = 1 \text{ mW/cm}^3$$

in the energy band 0.3 to 15 keV according to eq. (1). Assuming a parabolic temperature and a flat density profile, the detector receives a power from the central viewing chord (eq. (2))

$$P_D = 15 \ \mu\text{W},$$

which generates a signal current of

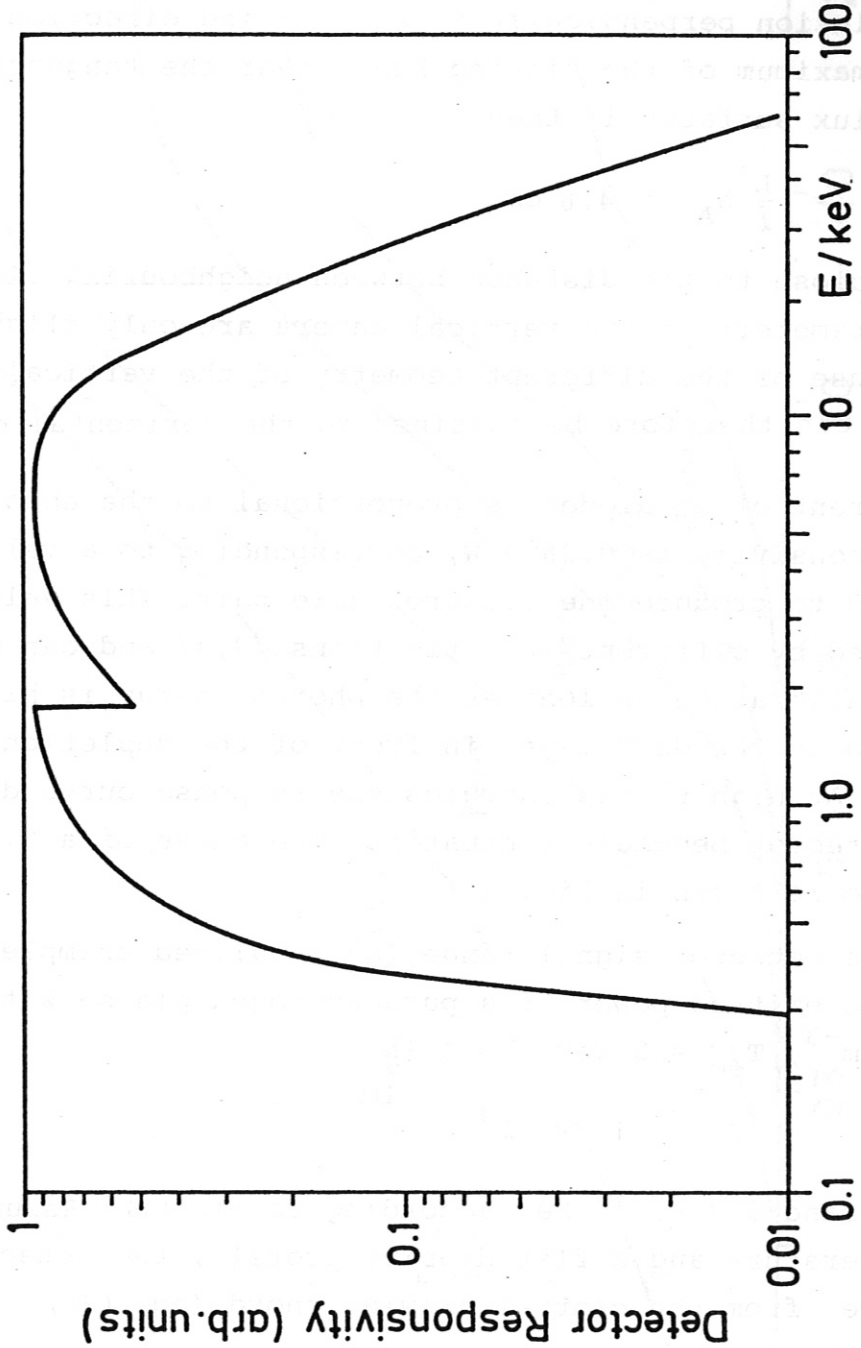

Fig. 3: Detector responsivity as a function of photon energy for a Quantrad PIN-Si diode of 300 µm thickness.

$$I_s = 4.2\ \mu A.$$

This current is 1000 times higher than the noise of the detector and preamplifier and can be regarded as an average signal. The power P_D = 15 μW corresponds to about 10^{11} photons of 1 keV energy per second, or 10^6 photons within 10 μs. So errors due to noise and photon statistics remain smaller than 0.1% for signals of this magnitude.

2.2.3 Range of Signals During H and D Phases of JET

According to JET Memo No.1 the JET plasmas will change their properties considerably during successive stages of H and D operation, and simultaneously the X-ray detector signal will vary by a factor of up to $3 \cdot 10^5$ in the most extreme cases. The power incident on the detector, calculated relative to the above example with equations (1) and (2), is summarized in the following table.

Table 1 Dynamic Range of Power Incident on the Detector

Parameter	Range according to JET Memo 1	X-ray power relative to example: 15 μW	Signal range in central channels
n_{eo}	1 to $8 \cdot 10^{13}$ cm^{-3}	1/10 to 7	10 nA to 3 mA
T_{eo}	0.4 to 4 keV	1/3 to 1	
ζ	1 to 100	1 to 100	
E_{min}	0.1 to 8 keV	1/10 to 1	
overall change	–	1/300 to 700	1 to $3 \cdot 10^5$

The table shows that signals in the central channels between 10 nA and 3 mA are possible. Near the plasma edge the signals will generally be about 100 times smaller. Even in the event that the most

extreme values are not reached, the large range cannot be covered by the detector and electronics. It is planned to start operation of the diagnostics with large apertures and to replace them by smaller ones when JET is opened for the installation of additional heating. Generally, thin filters can have a smaller opening than thicker ones, particularly those in front of central detectors. In the later stages of D-D operation of JET it seems preferable to replace thin filters by thicker ones whenever the cameras have to be demounted for any reason.

2.3 Effects of Neutron and Gamma Radiation

2.3.1 The Detector Problem

The parts most sensitive to neutron and gamma radiation are the detectors. Generally silicon surface barrier diodes are used in soft X-ray imaging diagnostics of present-day fusion plasmas. Unfortunately, these detectors cannot withstand temperatures higher than 40° C. JET requires that the cameras be taken to at least 150° C. Other detectors meeting the following requirements thus had to be sought:

- sensitivity as high as surface barrier detectors
- signal rise time $\leqq 10$ µs
- capability of measuring photon fluxes up to 10^{15} keV/s in the current mode (photon energy 0.5 - 15 keV)
- temperature during bake-out 150° C
- low sensitivity to magnetic fields
- high radiation damage threshold:
  $D_{tot} \approx 1000$ rad, $D_{\gamma} \approx 800$ rad, $D_n \sim 200$ rad $\hat{=} 4 \cdot 10^{12}$ n/cm^2
- operation at dose rates of up to
  $\dot{D}_{tot} \approx 0.5$ rad/s, $\dot{D}_{\gamma} \approx 0.4$ rad/s, $\dot{D}_n \approx 0.1$ rad/s
- availability for testing by 1982 at the latest for installation in 1984.

2.3.2 Shielding

The above levels of dose and dose rate are based on JET Memo No. 10. Allowance was made for additional shielding of the cameras by 25 - 30 cm Inconel. Unfortunately, no information on the directional distribution of the radiation could be provided by JET. Only a coarse design of the shielding and estimate of attenuation can therefore be made. An attenuation factor of 10 seems to be achievable. It is limited for three reasons:

- the space for shielding is rather limited
- the large viewing angle necessary for measuring the entire plasma leads to a large opening in the shielding
- the only material that can be used for shielding inside the JET vacuum was found to be Inconel. Other more efficient materials which could be covered by Inconel are either very expensive of cannot withstand temperatures of 400^{o} C.

Meanwhile it has been found that a shielding consisting of 10 to 20 cm of borated water followed by about 10 cm Inconel has very attractive properties. The water could be drained off during bake-out. The mass which has to be heated to the same temperature as the port is thus drastically reduced. An optional proposal for this type of shielding has already been announced to JET.

2.3.3 Investigations of Detectors

As detectors only Si diodes were found to be capable at least in principle of meeting the requirements stated in 4.1. Three types of Si diodes were therefore investigated in more detail:

a) Ion-implanted-Si diodes developed by the Technical University of Munich: Temperature allowed: 200^{o} C. Generally ideal properties for application (thin dead layer), but radiation hardness is low according to our tests. Attempts to improve the radiation hardness and initial tests have been started, but success is still uncertain.

b) Ortec ion-implanted-Si diodes: Temperatures of up to 200° C allowed. Very expensive. Up to now only circular detectors available; rectangular detectors will be supplied by Ortec if manufacturing turns out to be feasible. Radiation hardness of this specific detector has not yet been investigated.

c) Quantrad PIN-Si diodes: Temperatures of up to 150° C allowed. Specification of radiation hardness: 10^{12} n/cm^2 ≙ D_n = 50 rad, D_γ = 100 krad. This has been confirmed by a test of a single detector in the Neuherberg nuclear reactor. (For comparison an Ortec surface barrier detector was tested up to a dose D_n = 30 rad. The behaviour observed is similar to that of the Quantrad detector). Disadvantage: Because of a relatively thick dead layer the response to low energy X-rays is limited to $E > 0.6$ keV.

From these preliminary results the detectors produced by Quantrad are preferred. It is not yet certain, but probable, that measurements can be performed reliably up to an integrated dose $D_{n+\gamma}$ = 500 rad at the location of the detector. This corresponds roughly to half of the dose expected there during the H and D phases of JET. It is intended to continue these investigations. Probably a separate contract should be signed for this purpose.

2.3.4 Radiation-Generated Signals

The second aim of the detector tests performed was to measure the radiation-generated error signals occurring in the current mode operation:

a) n + γ generated increase of noise N $\propto$ (dose rate)$^{1/2}$

b) n + γ generated background signal $I_{BG} \propto$ dose rate

c) n + γ induced increase of leakage current $I_L \propto$ neutron dose.

As far as the detectors could be compared with respect to type, area and thickness, no major differences of these three parameters were found. In a good detector of 100 mm^2 area and 0.3 mm thickness

the following error signals have to be expected during a shot of JET producing $5 \cdot 10^{17}$ neutrons (JET Memo No. 10):

a) $N\ (10^5\ Hz) = 7\ nA_{rms}$ at $\dot{D}_{n+\gamma} = 0.5$ rad/s

b) $I_{BG} = 100$ nA at $\dot{D}_{n+\gamma} = 0.5$ rad/s

c) $\Delta I_{L,n} = 20$ nA after $D_n = 1$ rad

$\Delta I_{L,n} \gg \Delta I_{L,\gamma}$

At the end of the D-D phase of JET a leakage current of 4 μA would be expected theoretically. It has to be compensated electronically in order to preserve the dynamic range of the electronics and data acquisition.

2.3.5 Correction of Radiation-Generated Signals

These signals would lead to errors as large as 120 nA during the last high power DD discharges, corresponding to a relative error of 3% for a central channel signal of 4.2 μA and 300% near the plasma edge. These signals therefore have to be corrected. Five to ten additional detectors in front of which absorbers just thick enough to stop the X-rays up to 15 keV are placed will be provided in each camera.

A correction of the dominating $n + \gamma$ background signal I_{BG} with an accuracy of at least 5% ≙ 5 nA can be expected. The increase of leakage current, which may change considerably from detector to detector, will then produce an error not higher than 5 nA. At the average signal level of 4.2 μA, an overall accuracy better than 0,2 % in the central channel and 20% near the plasma edge can be achieved by means of this correction. This is a very conservative estimate, because the signal in the last DD discharges will be much higher than 4.2 μA. Perhaps the most severe situation may occur during the start of intense injection of neutral D into a relatively cold and clean D plasma with low X-ray emission. Careful checks

with the aperture of one camera closed will facilitate correct interpretion of the detector signals.

2.3.6 Preamplifiers

The preamplifiers are situated at the rear of the cameras and receive about the same dose as the detector. During detector tests preliminary preamplifiers were exposed to the same radiation field, and no important changes were observed. At present special electronic components, particularly the line driver, are under investigation.

3. Electronics and Data Acquisition

The general requirements for the Electronics and Data Acquisition System are:

- 100 electronic channels
- max. sampling rate 250 kHz
- resolution of the signals 12 bit
- sampling time 10 s.

All equipment necessary for the Electronic and Data Acquisition System will be located in the Diagnostic Area in Data Acquisition Cubicles. Only the preamplifiers are located at the back of the cameras.

3.1 Characteristics of the Electronic and Data Acquisition Channels

3.1.1 Overview

The main elements of the electronic channels are:

- detectors
- preamplifiers
- main amplifiers
- filters
- analog digital convertors
- optocouplers
- memories (RAM)

The scheme of the system is shown in Fig. 4.

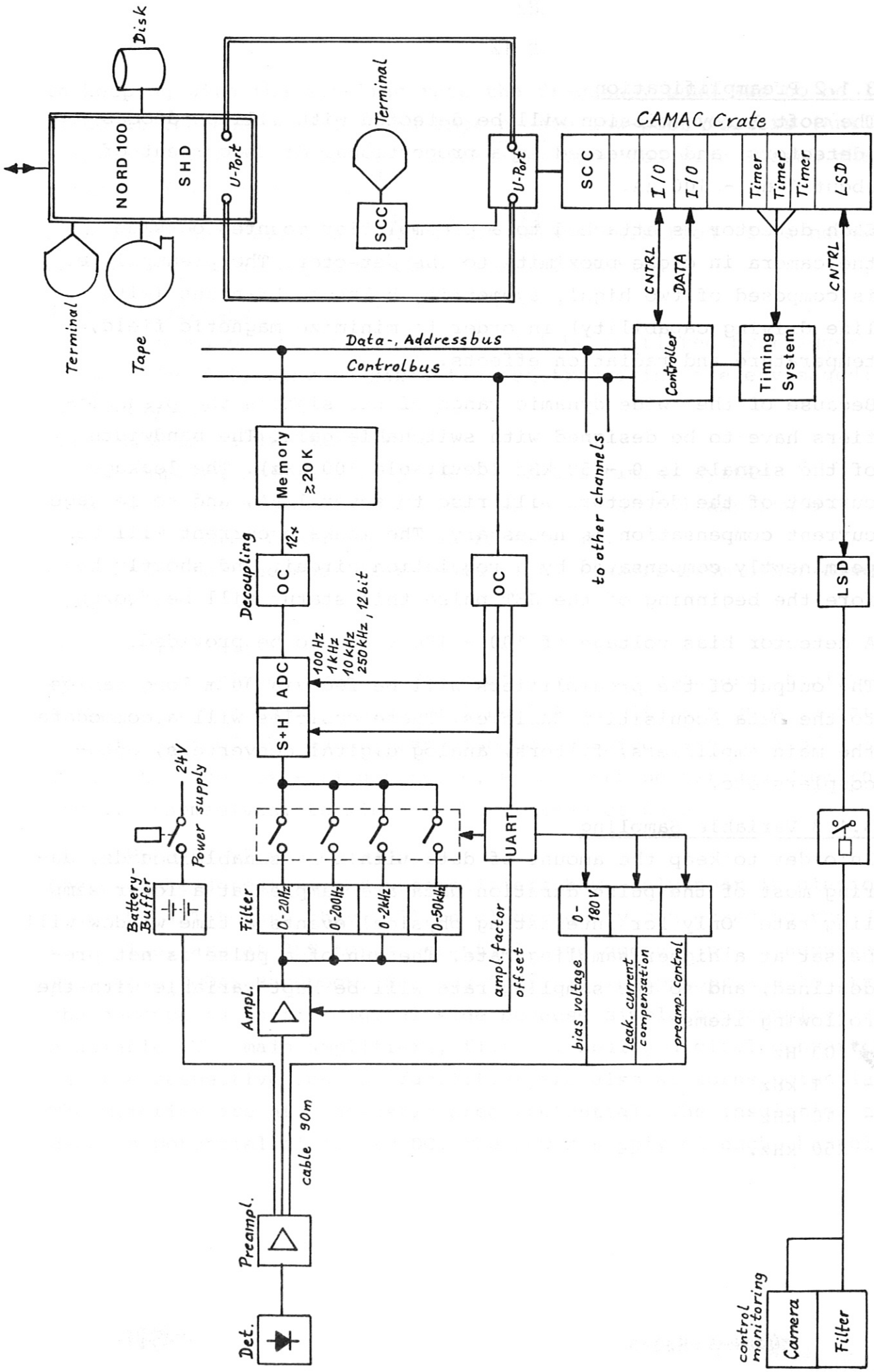

Fig. 4: Electronics and Data Acquisition with Analog Filtering

3.1.2 Preamplification

The soft X-ray emission will be detected with silicon diodes (detectors) and converted to a proportional diode current of about 1 nA - 100 µA.

Each detector is attached to a preamplifier mounted outside the camera in close proximity to the detector. The preamplifier is composed of two highly symmetric, balanced branches (with line driving capability) in order to minimize magnetic field, temperature and radiation effects.

Because of the wide dynamic range of the signals the preamplifiers have to be designed with switchable gain. The bandwidth of the signals is 0 - 50 kHz (desirable 100 kHz). The leakage current of the detectors will rise to several µA, and so leakage current compensation is necessary. The leakage current will be permanently compensated by a regulation circuit and shortly before the beginning of the JET pulse this status will be frozen.

A detector bias voltage of 100 - 180 V has to be provided.

The output of the preamplifiers will be fed via 90 m long cables to the Data Acquisition Cubicles. These cubicles will accommodate the main amplifiers, filters, analog digital converters, optocouplers etc.

3.1.3 Variable Sampling

In order to keep the amount of data within reasonable bounds, during most of the pulse duration data are sampled at a lower sampling rate. Only for interesting physical events a time window will be set at a higher sampling rate. The run of a pulse is not predestined, and so the sampling rate will be kept variable with the following items:

- 100 Hz
- 1 kHz
- 10 kHz
- 250 kHz.

In keeping with the sampling rate the frequency band has to be limited at the analog side with appropriate low-pass filters (Anti-aliasing). For this purpose filters are provided with Bessel characteristic (linear phase).

Because of the variable sequence of data acquisition it is necessary to reserve one memory for coded time information.

3.1.4 Triggering

The switching of the sampling rate will be initiated by trigger pulses. The following possibilities of triggering are envisaged:

Pre-triggering:

There are three different types:

- the sampling sequence is preset in the timing system
- the sampling sequence is changed when the signal amplitude within certain frequency bands is exceeded
- the sampling sequence is changed with triggers from other diagnostics.

Post-triggering:

In the post-triggering-mode the memory will be used essentially as as pass-through memory which will be filled with a high data rate. A small part of the memory can also be occupied with data of a lower data rate. The post-trigger pulse, which will be derived from the signals themselves, terminates the storage of data.

3.1.5 Decoupling and Insulation

Because the detectors and preamplifiers have only poor insulation from the JET torus, they will be electrically connected to the device. They are at JET torus potential, and decoupling is necessary (see also CODAS Handbook, Section 5.2). It is appropriate to arrange the decoupling on the digital side because simple optocouplers are available. The main amplifiers, filters, analog digital converters and the respective control facilities are also at torus potential. The memories are at Diagnostic Area potential. The insulation exceeds a potential of 1.5 kV DC. The power supply of each channel

shall be battery buffered. During the JET pulse the feed line is disconnected in order to break loops.

3.1.6 Main Amplification

The main amplifiers have remotely switchable gain in order to produce output which fits the requirements of the data acquisition system. The overall gain of the amplification will range between 1 and 1000.
In connection with the leckage current compensation of the detectors the amplifier offset is adjusted automatically.

3.1.7 Data Acquisition

After digitalization the data are stored in memories. The writing into the memories is parallel for the 100 channels during the pulse; reading of the 100 memories after the pulse has to be serial, this being done with the CAMAC Serial Highway with a lower data rate (max. 50 kwords/sec). The interface is a CAMAC-I/0-Module (HYTEC 440X-6), which works by a handshake procedure.

3.1.8 Data Amount

A data amount of about 20 kwords (12 bit) per detector and per pulse is envisaged. This provides a total data amount of 2 Mwords per pulse.

3.2 Remote Control of Electronics

Remote control of electronics by terminal only occurs between pulses. The following tasks have to be done:

- adjustment of the bias voltage of the detectors
- monitoring of the detector current
- compensation of the leakage current of the detectors
- disconnecting of the bias voltage in the event of short-circuiting of a detector (the detectors should always be connected with bias voltage; only during the baking phase or discharge cleaning must the bias voltage be disconnected)
- switching of the gain of the preamplifiers and main amplifiers (separate for each amplifier, but preferably program-controlled)

- automatic offset control for all main amplifiers
- preselection of the trigger mode, programming of the timing system
- testing of the diagnostic arrangement (occasional); a light source is mounted in the camera box to provide a means for testing the detector and the electronics.

The control commands and replies will be interfaced with a CAMAC-I/0-Module (HYTEC 440X-6).

3.3 Remote Control for the Cameras

In each camera there are devices which must be controlled and monitored.

Control only occurs between pulses.

In detail, the following functions are envisaged:

3.3.1 Horizontal Camera

1 filter wheel with 5 positions
2 filter bands with 4 positions each
3 cooling circuits
8 heater elements
1 test light
6 sensors for monitoring of temperature
1 sensor for monitoring of vacuum
2 sensors for monitoring of air pressure.

3.3.2 Vertical Camera

1 filter wheel with 5 positions
1 filter band with 3 positions
3 cooling circuits
4 heater elements
1 test light
6 sensors for monitoring of temperature
1 sensor for monitoring of vacuum
2 sensors for monitoring of air pressure.

3.3.3 Control and Monitoring

In order to manage the camera control and monitoring there are different types of single bit signals:

- control commands
- status signals
- failure signals.

The control commands are output signals for ON-OFF control of the equipment.
The status signals are input signals to indicate the status of the equipment.
The failure signals are input signals to indicate failure of power, interruption of circuits, exceeding of limit values etc.

In the case of one horizontal and one vertical camera the following approximate numbers of single bit signals are required:

- 59 control commands
- 59 status signals
- 64 failure signals.

The single bit signals will be interfaced to the CAMAC Dataway by the Line Surveyor Driver (LSD).

The sensors for temperature and vacuum provide analog signals to regulate the heating/cooling and vacuum systems. These values can also be transferred to the CAMAC Dataway.
There are 14 analog indications. They will be interfaced by a Scanning ADC 16 ch. slow (LeCroy 8216).

3.3.4 Interlock

The heating/cooling system must work during baking and discharge cleaning of the torus. The filter wheel must be in the position of the thickest filter when the diagnostic is not in operation, particulary during baking and discharge cleaning. During the measurements the detector temperature has to be kept below 25^{o} C.

3.4 Cables

For the connections between the preamplifier and junction box and

between the junction box and Diagnostic Area the following type of cable will be used:

FC No. E014:
2 quad cable
JET type L093
4 symmetrically twisted wires per quad
wire cross-section 0.2 mm^2
every quad screened with copper braid
common screen with copper braid
test voltage 2 kV dc.

For connections in the junction box a LEMO Size 3 connector (10 pins) will be used.

3.5 List of devices to be delivered by JET

1 CAMAC Crates CPC1	Grenson
1 Crate Controller CCC2	Fisher 2401
2 I/0-Module, 16 bit CPR1	HYTEC 440X-6
1 LSD Module CLS2	Sension
3 Timer Sys Module CTM1	Sension 1352
1 Stopwatch CTM2	Sension 1371
1 Multi-channel DAC CDA2	HYTEC 640 V(s)
1 Scanning ADC 16 ch. CAD 1	LeCroy 8216
1 LSD Subrack UCB2	Sension
1 LSD Connector Card ULC1	"
1 LSD Power Supply Unit UPS1	"
8 LSD Input Card ULS1	"
4 LSD Output Card ULD1	"

6 Cubicles with Euro-Card-Racks 19" and Power Supplies

1 Magnetic tape recorder for archiving,
e.g. EMI SE7000C 14 Tracks

3.6 Electronics and Data Acquisition with Digital Filtering

In principle, there is a possibility of realizing the change of bandwidth and sampling rate by digital filtering. A block scheme is shown in Fig. 5. This would have the advantage that a set of data recorded with the highest frequency and stored in a small buffer can be checked for its information content before the decision on bandwidth reduction has to be made. Particularly the post-trigger mode will be much more effective. In addition, digital filters have technical advantages over analog filters: Their properties are not dependent on the temperature, tolerance and age of the components. The channel-to-channel differences are therefore minimized.

It is not yet quite sure whether such a system is feasible. The problem is the high processing speed required for the high sampling rate. This point is being investigated at the moment and an answer is expected within two months. If a solution can be achieved, a system with digital filtering will be proposed to JET.

3.7 Data Analysis

After the pulse the subsystem computer has to execute the following tasks:

- reading the memories via CAMAC Serial Highway and data storage on disk
- transfer of the data to CODAS pulse file and selection of interesting data, if desired
- correction and evaluation of the data, Abel inversion
- plot of flux, emission and temperature profiles, three-dimensional plots
- archiving on tape.

The capacity of the disk should be large enough for the pulses of about one day or more.

A tape recorder for long-time storage must be attached to the

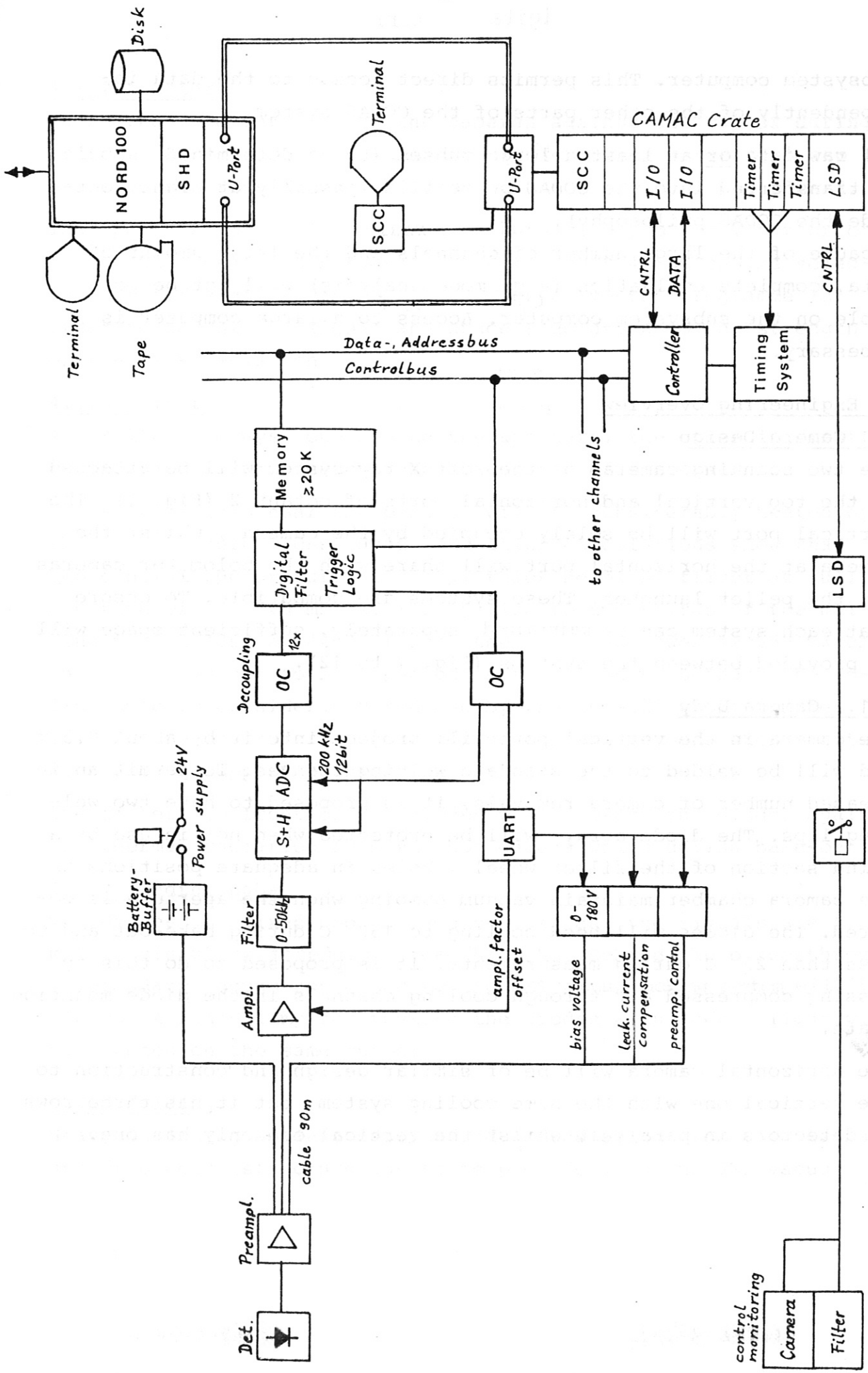

Fig. 5 : Electronics and Data Acquisition with Digital Filtering

subsystem computer. This permits direct access to the data independently of the other parts of the CODAS system.

All raw data or at least a large subset (to be determined) should be transferred into the CODAS pulse file (possibly at night, outside the CODAS philosophy).
Because of the large number of channels and the large amount of data, complete evaluation (e.g. mode analysis) will not be possible on the subsystem computer. Access to a large computer is necessary.

4. Engineering Overview

4.1 Camera Design

The two scanning cameras of the soft X-ray system will be attached to the top vertical and horizontal ports of octant 2 (Fig. 1). The vertical port will be solely occupied by the camera , whilst the camera at the horizontal port will share with the bolometer cameras and the pellet launcher. These systems are compatible. To ensure that each system can be maintained separately, sufficient space will be provided between the systems (Fig. 7 to 12).

4.1.1 Camera Body

The camera in the vertical port will project into it by about 0.5 m and will be welded to the standard welding flanges. To permit an increased number of camera removals, it is proposed to have two welding lips. The diode array will be protected when not in use by a blind section of the filter wheel . Holes in adequate positions in the camera chamber maintain vacuum pumping when the aperture is covered. The diodes will need cooling to 150^{o} C during bake-out and to less than 25^{o} C during measurements. It is proposed to do this by passing compressed air through cooling channels in the diode mounting plate.

The horizontal camera will be of similar design and construction to the vertical one with the same cooling system, but it has three rows of detectors in parallel, whilst the vertical one only has one.

4.1.2 Aperture

To protect the interior of the cameras against the vapour during the procedure of cleaning the torus interior, a watertigth cap will be fixed in front of the aperture by means of a knuckle thread.

The aperture mount can be manually replaced from the interior of the torus. Apertures between 5 x 20 to 20 x 40 mm^2 can be selected for different stages of the JET experimental programme in order to adjust the signal and space resolution to the strength of the X-ray emission.

4.1.3 Filters

The filter arrays, one behind the aperture, the other in front of the diodes, are the only movable parts of the cameras.

The thin filters near the pinhole will be considerably heated by the plasma energy loss. Heat conduction calculations show that the central temperature of a 1 µm thick Be or Al filter at full aperture of 20 x 40 mm^2 will only rise to two-thirds of the melting points (860 or 440^{o} C) when the absorbed power is 250 mW/cm^2. This value is not to be expected in the DD phase because the solid angle is considerably reduced by the shielding. If thinner filters are desired, the heat conduction can be made about 10 times higher by a supporting nickel mesh.

The filters in front of the diodes will protect the diodes against the thermal radiation from the hot camera walls during bake-out.

4.1.4 Feedthroughs

The diodes are fixed on a curved support and the signals are transmitted via glass imbedded feedthroughs. Behind these feedthroughs a secondary vacuum connected to the JET vacuum backing system will be placed. A flash lamp for testing the diodes with visible light will be mounted on the same support.

4.2 Shielding

Heavy shielding against neutron and γ-radiation from the plasma and the machine structure has to be provided. In the JET vacuum

the material has to be Inconel. For outside lead, stainless steel and polyethylene are being considered. The thickness has to be 150 - 250 mm. Cooling and heating are required at least for the part inside the port.

4.3 Remote Handling

The diagnostic is expected to operate only in the DD phase of JET owing to radiation damage to the diodes. Repairs therefore do not need to be made by RH. The possibility of disconnecting the cameras as a whole from the torus by RH during the DT phase is kept open. The lifting capacities of the overhead crane (150 tons) and of the servo manipulator (25 kg) will be considered.

All service connectors such as compressed air and electricity will be JET-standard types as also will be the flanges from the prevacuum to atmosphere, where glass feedthroughs will be used. The whole system is classified as RH class 3 (see Appendix 1).

4.4 Specification of the Interface with the JET Torus Vacuum System

4.4.1 Scope

This note defines the interface between the diagnostic system and the JET torus vacuum system. It also provides a preliminary description of the design, fabrication details, tests and vacuum standards of the components associated with the vacuum interface.

4.4.2 General Remarks

The X-ray diodes will be connected directly onto the JET torus vacuum system and there is no provision for isolating valves. The cameras must therefore be constructed to the highest vacuum standards and their design must be consistent with the vacuum standards of the JET torus vacuum itself.

Care will be taken during design to avoid trapped volumes with a considerably longer pump down time constant than the torus (torus = 10 seconds). The internal surface area of the units will be kept to a minimum. All materials are approved by JET for the bolometer diagnostic, except Be and the flash bulb.

Outline of the Vacuum Interface

The interface problems between the diagnostic and the JET torus vacuum system concern the following:

construction materials
vacuum connections
movable filter arrays
bake-out and cleaning procedures
welding

4.4.3 Contruction Materials

The following materials are proposed for the construction of the cameras:

I Camera bodies and shielding
Vacuum melted Inconel 600 is proposed for the construction of all parts for the vacuum bodies of the cameras and for the shielding.

II Ball bearings are required for the movable filter supports (steel AISI 440 C, without lubricant).

III Glass imbedded feedthroughs are used to make electrical connections into the vacuum for the detectors.

IV The pins of the feedthroughs will be made from platinum-iridium (95 % - 5 %).

V The twisted cables between the detectors and the preamplifiers will be Kapton-insulated. However, these cables are in the prevacuum and together with the connectors to atmosphere in a region with temperature beyond 150^{o} C.

VI The flash lamp is not yet specified. The bulb will be made of glass or fused quartz.

VII Diodes

a) The detectors themselves are not yet specified.
b) Aluminium (AlMg3) is used for the diode element housing (each is approximately 38 x 16 x 15 mm).
c) Beryllium-copper is required for the electrical spring contacts of the detector (2 springs per element body).

d) Machinable glass ceramic (MACOR) is required for the spring contact support system.

e) Kapton is used as insulating material for the detector housing. It is almost totally covered, only 120 mm^2 on each detector is exposed to the vacuum.

f) The materials of the filters will be beryllium and aluminium. The surface exposed to the vacuum will be: horizontal camera about 500 cm^2 beryllium and aluminium each; vertical camera about 100 cm^2 beryllium and aluminium each.

Published data on kapton polyimide foil[5] indicate a very low outgassing rate ($< 1 \times 10^{-12}$ torrl/s/cm^2) on reaching room temperature after bake-out to 300° C for 5 1/2 hours (see Fig. 6a). This source gives no information, however, on the residual gas composition of the outgassing. Varian data [6] for Vespel polyimide in the form of gaskets for vacuum valves indicate a higher outgassing rate after bake-out to the same temperature (see Fig. 6b), but there appear to be some property differences between the two materials (the gas permeability, for example, is higher for Vespel[7]). Residual gas analysis on Vespel at 300° C[6] indicates that the principal gases involved are water vapour, carbon monoxide, carbon dioxide and hydrogen (nothing appears above mass 44[8]). When restored to room temperature, the water vapour was no longer detectable and the primary gases were then found to be carbon monoxide and carbon dioxide. It therefore appears that although polyimide is a hydroscopic material, water vapour is removed by bake-out.

Kapton is bakeable to 300° C but the temperature of the insulation foils will be limited to a temperature of about 150° C owing to the cooling of the diode support plate. The total surface area of exposed kapton is about 150 cm^2 (contained in two cameras) so that the total impurity flux determined from the specific outgassing rate data in Ref. 6 would be $\sim 1.5 \times 10^{-10}$ torrl/s after bake-out to 300° C. This value will be higher if the bake-out is limited

MACOR AND POLYIMIDE OUTGASSING DATA

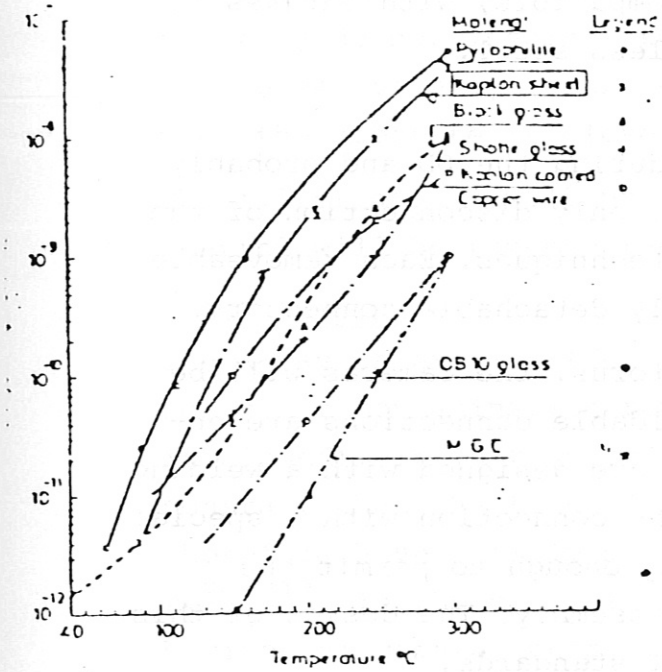

Fig 6a Outgassing rate of 7 materials as a function of temperature.

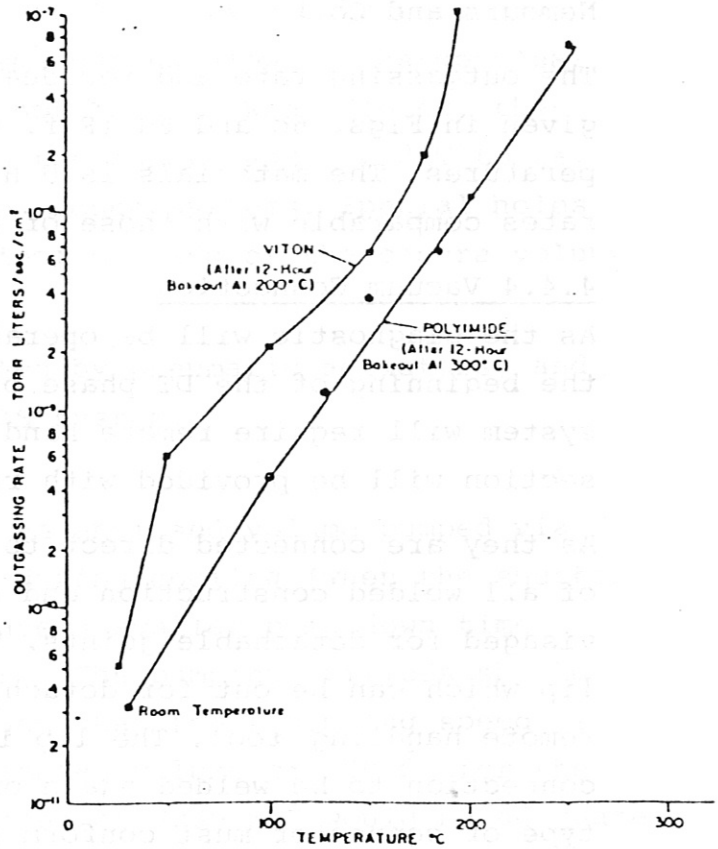

Fig 6b Outgassing rates of Viton A and polyimide

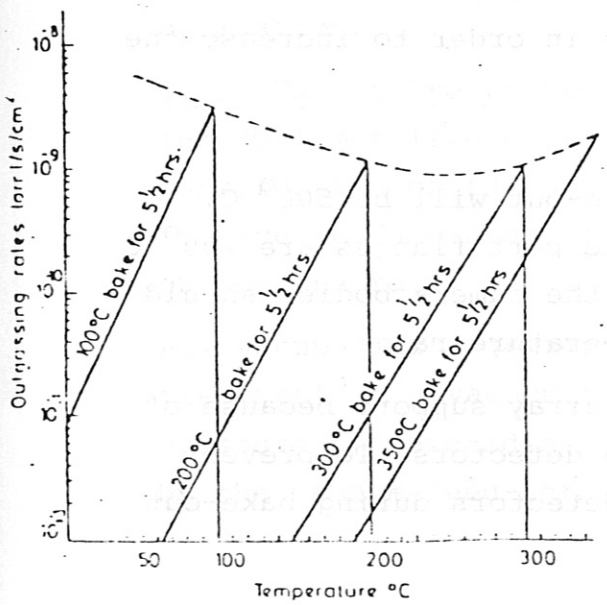

Fig 6c Outgassing rate as a function of temperature for machinable glass ceramic. (MACOR)

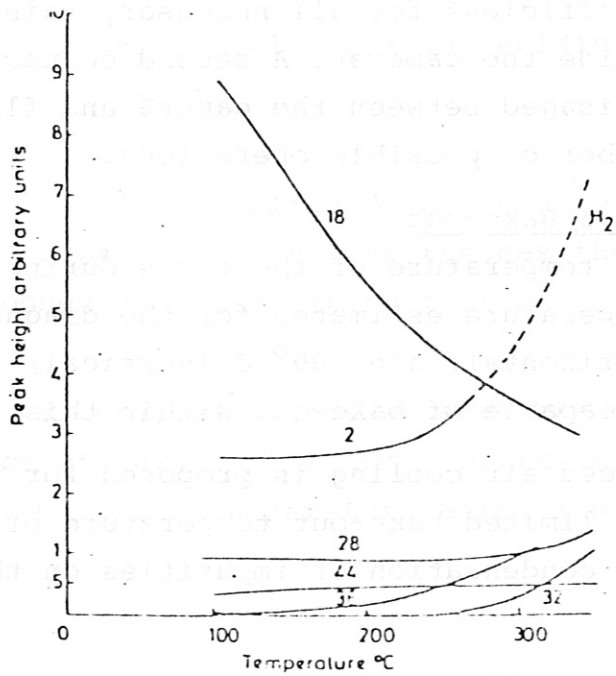

Fig 6d Residual gases as a function of temperature for machinable glass ceramic.

to 150° C, but probably not greater than by a factor of 100. Measurements will be performed at Garching to confirm this value. (Note: Kapton and Vespel are trade names of E.I.Du Pont Nemours and Co.)

The outgassing rate and residual gas composition for Macor are given in Figs. 6c and 6d (Ref. 5), after bake-out to various temperatures. The materials is U.H.V. compatible, with outgassing rates comparable with those of stainless steel.

4.4.4 Vacuum Connection

As the diagnostic will be operating during the DD and probably the beginning of the DT phase of JET, only disconnection of the system will require remote handling techniques. Each removeable section will be provided with remotely detachable connectors.

As they are connected direct to the torus, the cameras will be of all welded construction and re-weldable connections are envisaged for detachable joints. These are designed with a welding lip which can be cut for detaching the connection with a special remote handling tool. The lip is long enough to permit the connection to be welded again on re-assembly. The design of this type of connector must conform to JET standards.

The limited number of 3 - 4 rewelding operations is estimated as insufficient for all necessary maintenance and repair operations inside the cameras. A second connector in series is therefore envisaged between the camera and flange in order to increase the number of possible operations.

4.4.5 Bake-out

The temperature of the torus during bake-out will be 500° C. Temperature estimates for the diagnostic port flanges are 400° C (horizontal) and 300° C (vertical) and the camera bodies should be capable of bake-out within this temperature range.

Forced air cooling is proposed for the array support because of the limited bake-out temperature of the detectors. To prevent the condensation of impurities on the detectors during bake-out

their minimum temperature should not be less than 150^{o} C.

4.4.5 Movable Filters

The filters will protect the detectors against radiant heating from the torus and the hot camera walls during bake-out, and against deposition from the plasma during glow discharge cleaning and when the diagnostic is not in use. When closed, they restrict the conductance between the camera and the JET torus, but they do not insulate the two vacuum systems. Special holes in the camera body ensure efficient pumping of the camera volume when the aperture is closed.

The filter arrays will be operated by pneumatic actuators, and control will be through the CODAS system.

4.4.7 Pumping

The X-ray camera is effectively an enclosed volume pumped via holes for contamination removal during cooling (when the shutter is closed). It is required to have a smaller pump down time constant than the torus ($<$ 10 s). The pumping orifices should therefore have a minimum area such that their pumping speed is $\sim\frac{\text{volume}}{10}$. In the case of an estimated volume of 180 ℓ for the horizontal camera, pumping orifices of 3200 mm^2 would be adequate (e.g. 10 holes of 10 mm radius).

4.4.8 Welding

Appendix A is provided as a typical example of a UHV welding specification.

4.4.9 Vacuum Treatments

Internal metallic parts will be electropolished, preferably after construction of the particular part. The process reduces the effective surface area of components, thus helping to reduce the outgassing rate.

All vacuum parts (except the diodes) will undergo pre-bake-out treatment in a vacuum furnace at max. 300^{o} C for 3 hours at a pressure not exceeding 10^{-5} mbar, the temperature being limited by the vacuum feed-throughs.

4.4.10 Cleaning

Appendix B is provided as a typical UHV cleaning specification.

4.4.11 Special Conditions

In addition to the UHV requirement, the following special conditions will need to be met:

Use of Tritium

The use of tritium during experiments requires special precautions in the choice of materials used in construction. Materials that might undergo property changes which are crucial to their function (e.g. elastomers, oils, plastics, etc.) will be avoided.

Furthermore, the use of tritium requires the installation of metal seals to the atmosphere and certain standards of vacuum tightness as specified in paragraph 11.

Radiation

All materials except the detectors and preamplifiers are capable of withstanding an accumulated total radiation dose of 10^8 rad with negligible effect on their proper functioning or reliability.

Vibration

Components mounted direct to the JET torus will be subjected to mechanical shock due to major disruptions of the discharge which are expected to be relatively infrequent. A shock acceleration of approximately 150 ms^{-2} in 3 ms is estimated for JET.

Stray Magnetic Fields

During a plasma pulse magnetic fields of approximately 4000 gauss will exist in the region of the main vertical and horizontal ports. Components will therefore be made of non-magnetic materials.

4.4.12 Vacuum Tests

Leak Tests

The total leak rate of the camera bodies should be $\leq 10^{-9}$ mbar l/s, when enclosed by a container filled with helium gas (1 bar). The measurement will be performed at room temperature and at a temperature of not less than 150^{o} C.

Impurity Test

Each completely assembled camera unit will be mounted in a vacuum chamber by its vacuum flange and submitted to a simulated torus port bake-out (with cooling on the diodes). A residual gas spectrum will be made both before and after bake-out to determine the impurity partial pressure produced by the system.

Acknowledgements

The authors are pleased to acknowledge the support by the members of the X-ray diagnostic groups in the IPP. In particular the numerous discussions with Dr.P.Smeulders and Dr.K.Hill were very helpful in finding the present design of the diagnostic system. We appreciate very much the contributions of Dr.H.Krause, who performed the shielding calculations. We thank Mr.D.E.Groening for many valuable advices and Mr.D.Gonda and Mr.J.Hausmann for continuing technical assistance.

References

(1) S. von Goeler et al., Nucl. Fusion 15, 301 (1975)
(2) Report: Bolometry for JET, IPP Garching, 1981
(3) R.Petrasso et al., Rev. Sci. Instrum. 51 (5), 585 (1980)
(4) H.Büker, Theorie und Praxis der Halbleiterdetektoren für Kernstrahlung, Springer Verlag 1971
(5) Vacuum Design and Discharge Cleaning in Large Pinch Experiments, L.Firth, F.C.Jones and A.A.Newton, Culham Labs.
(6) The Application of Polyimide to Ultra-high Vacuum Seals, P.Hait Varian Ass., Vacuum 17, number 10, p. 547 (1967)
(7) Permeating and Outgassing of Vacuum Materials W.G.Perkins, J. Vac. Sci. Technol. Vol. 10, No. 4, July/Aug. 1973
(8) Polyimide Characteristics - Varian Ass.

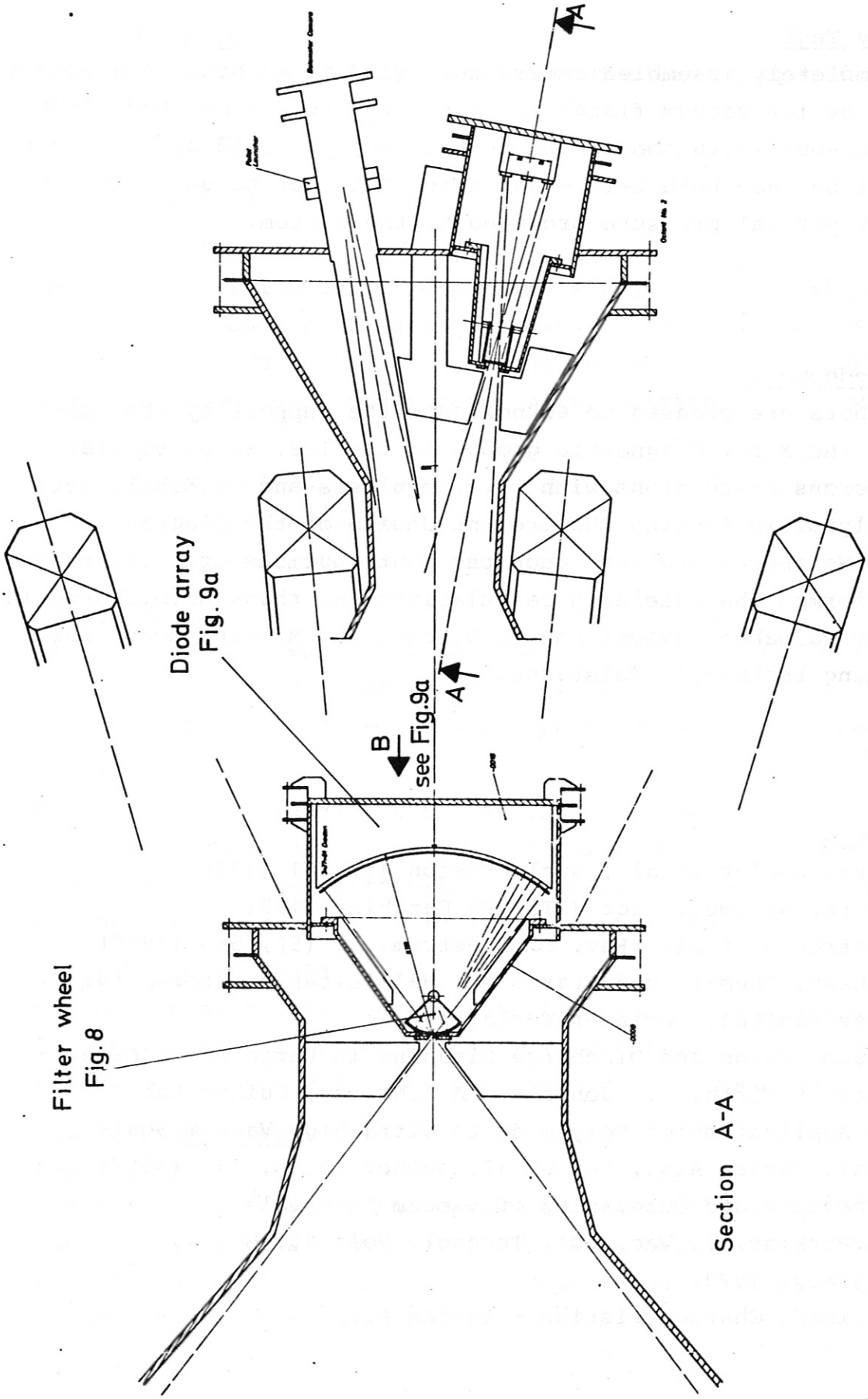

Fig. 7
Horizontal camera
(schematic)

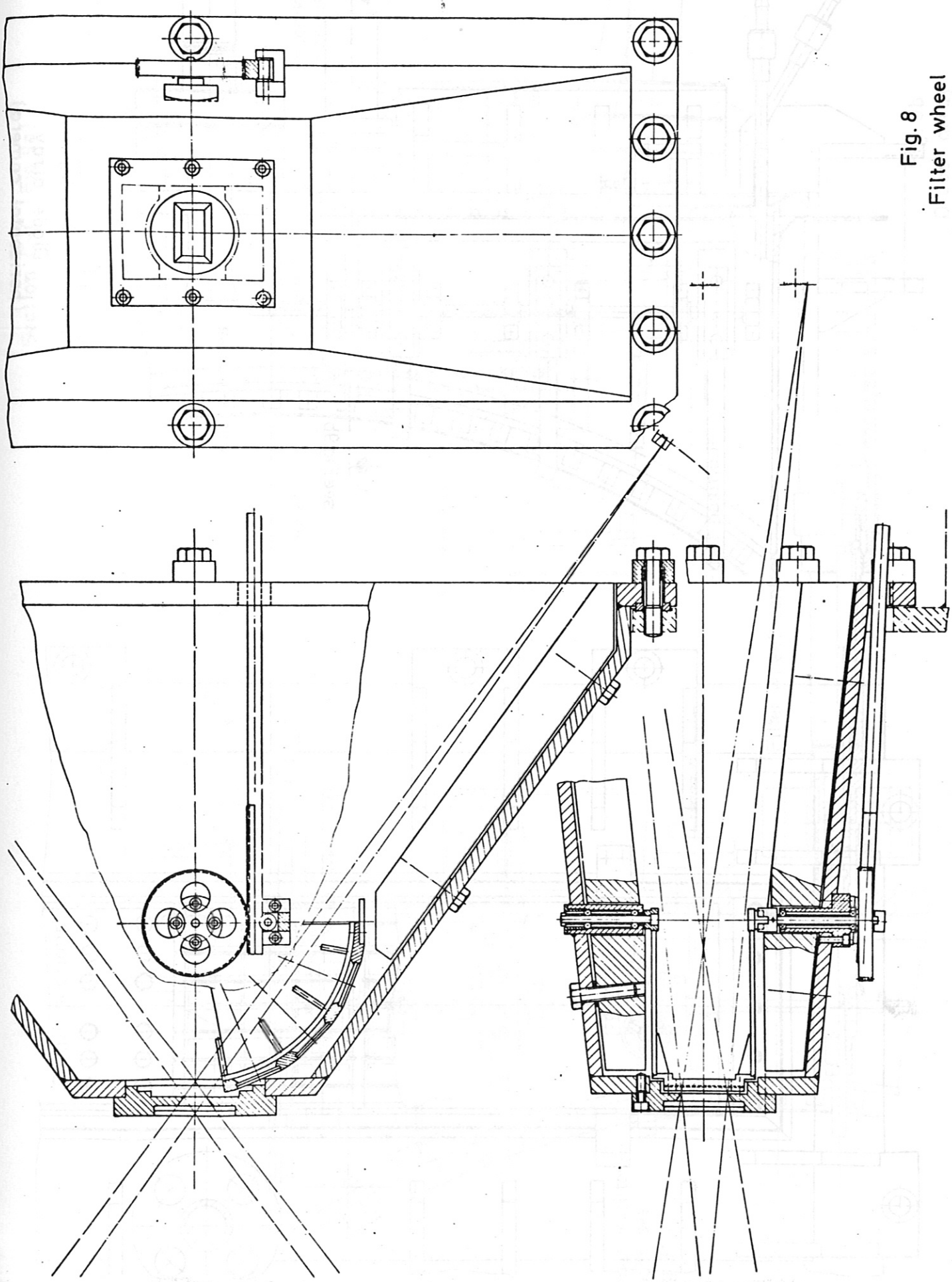

Fig. 8
Filter wheel
(horizontal camera)

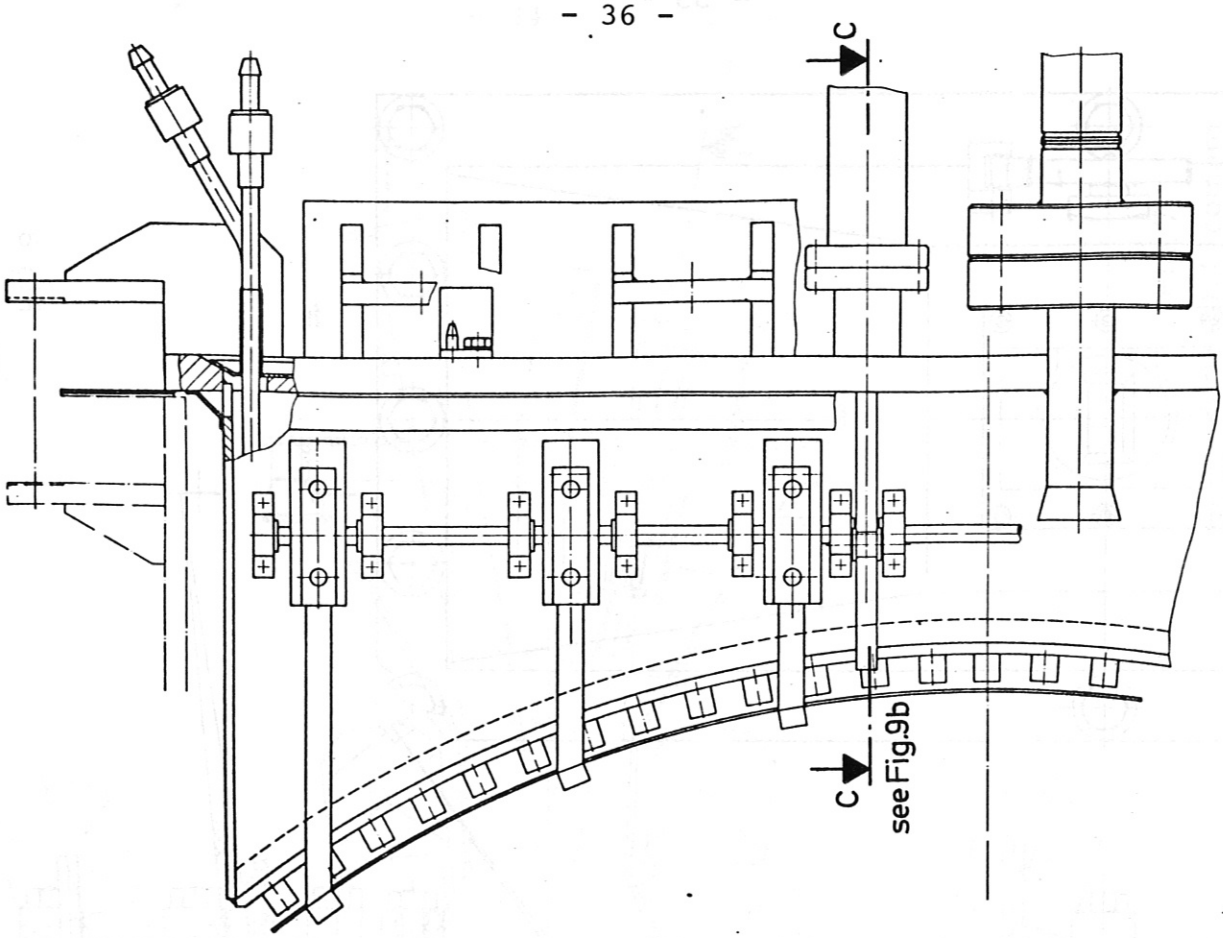

Fig. 9a
Diode array
(horizontal camera)

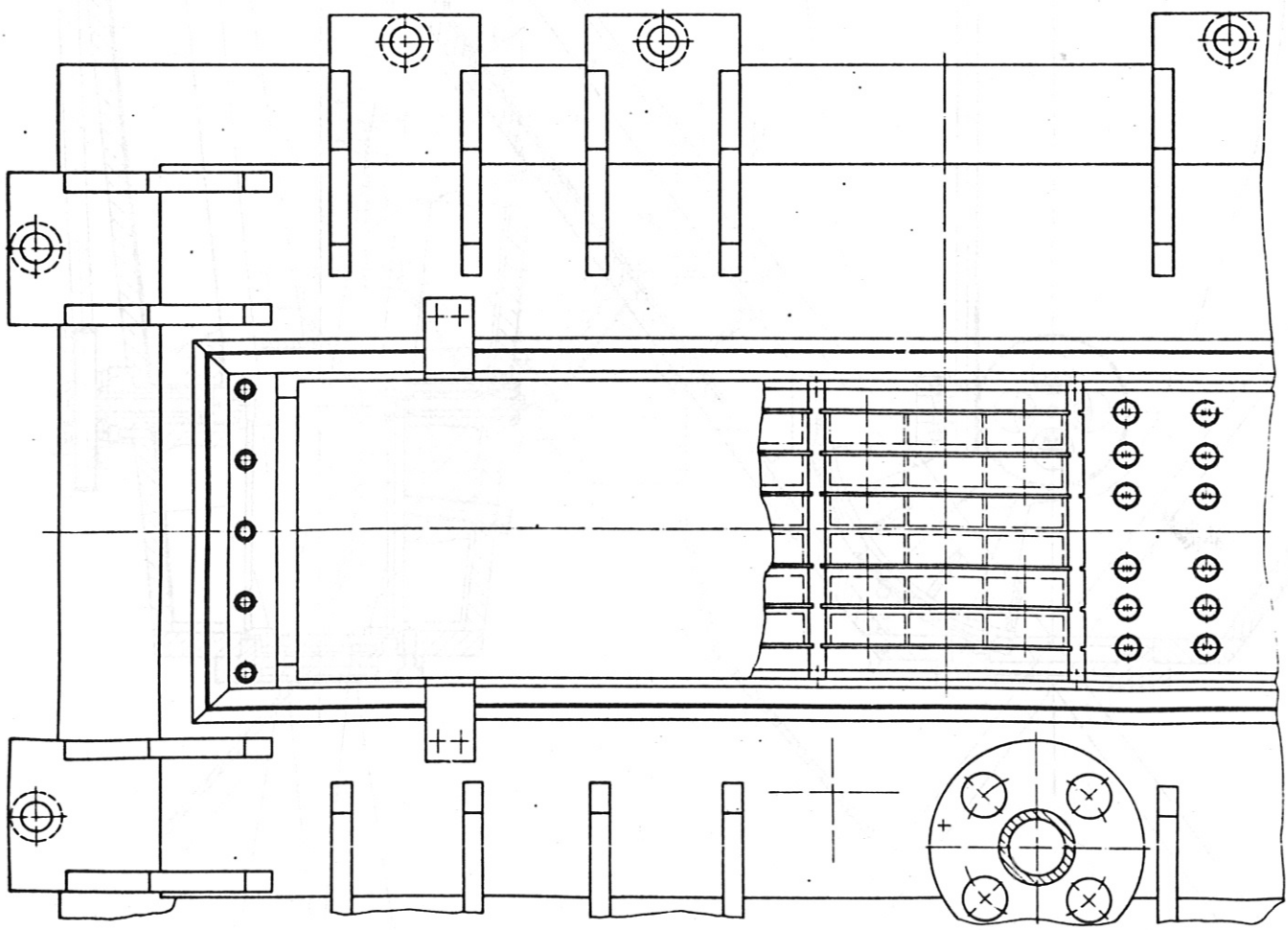

View in direction B (Fig.7)

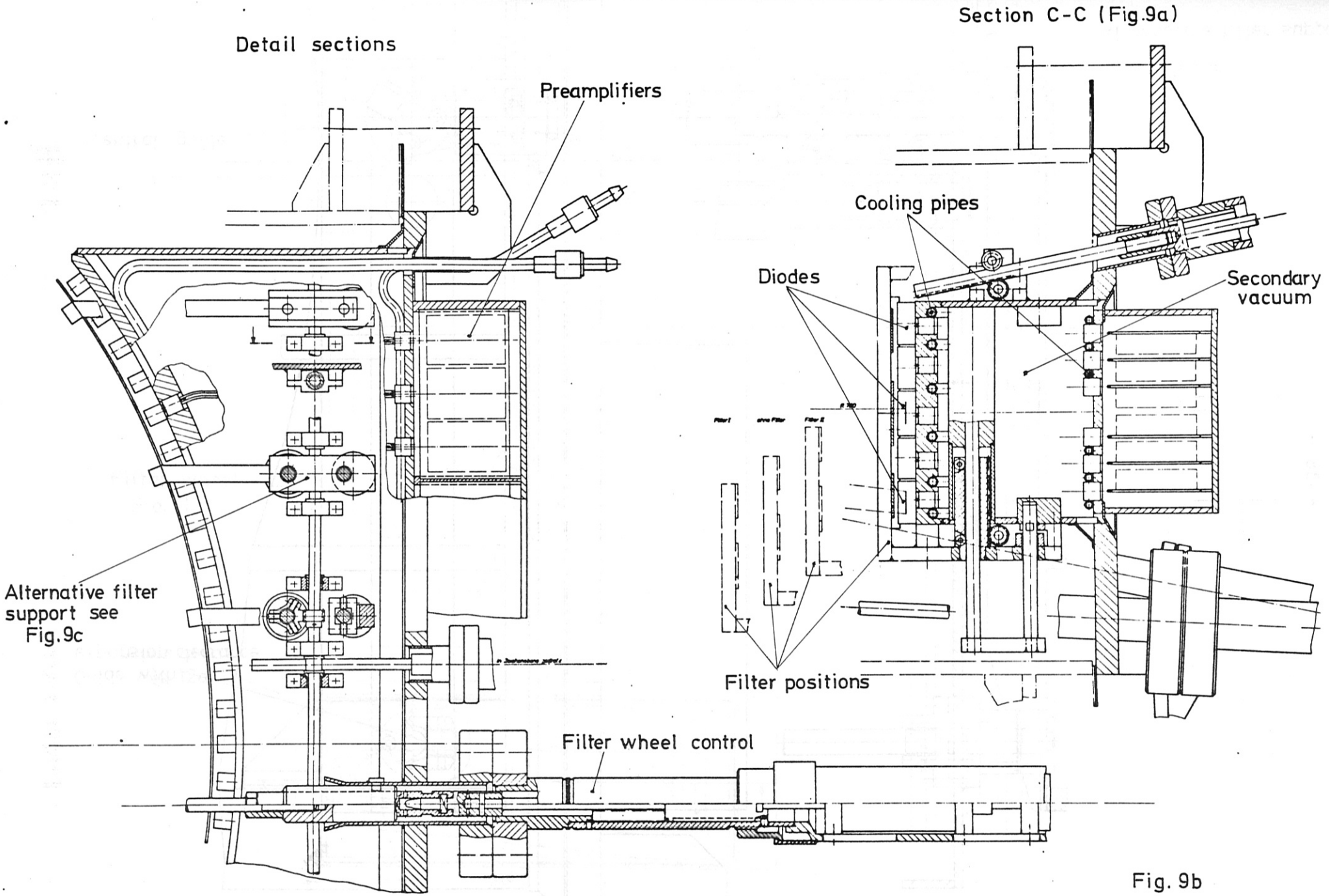

Fig. 9b
Diode array
(horizontal camera)

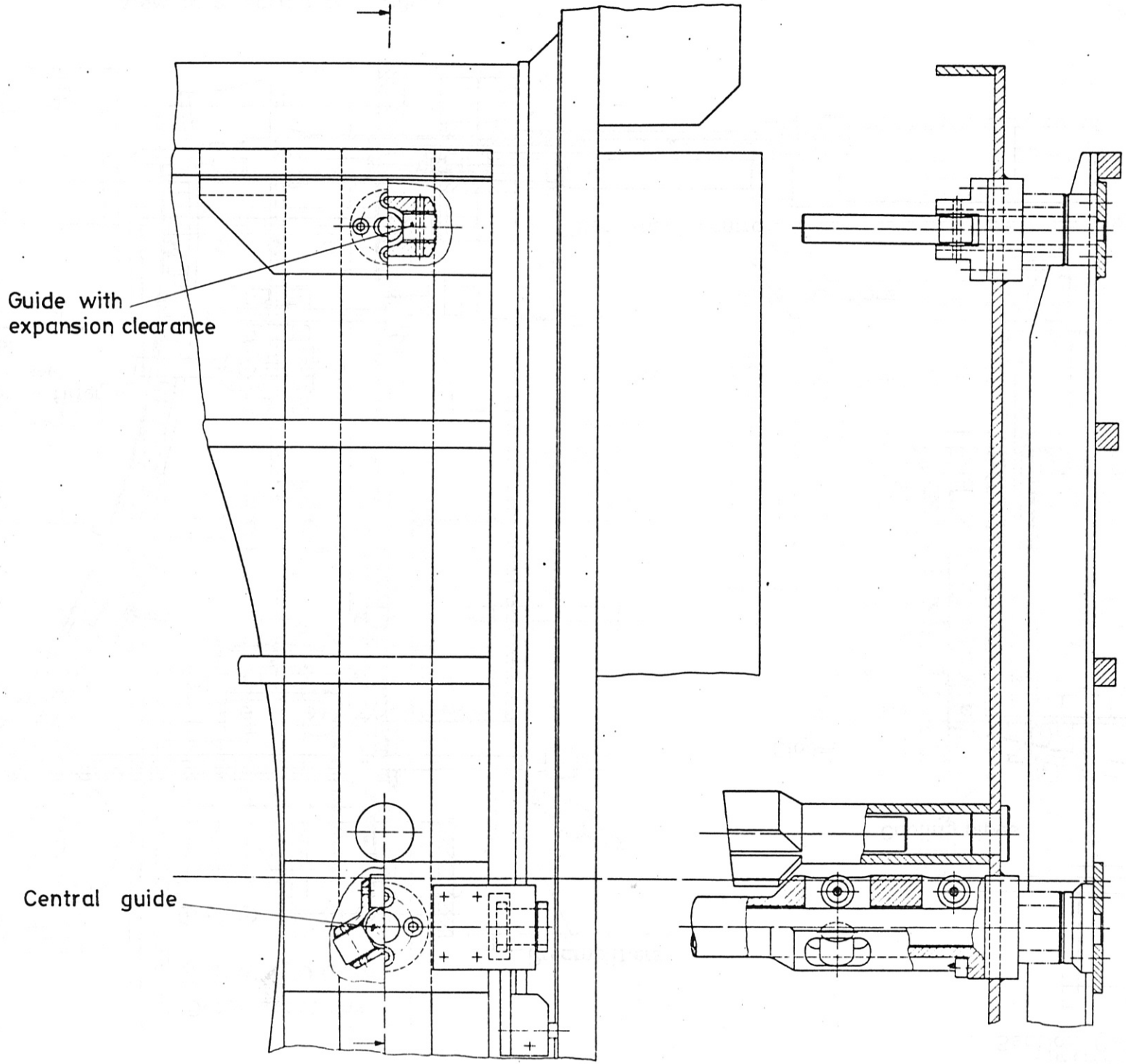

Fig.9c
Alternative filter support

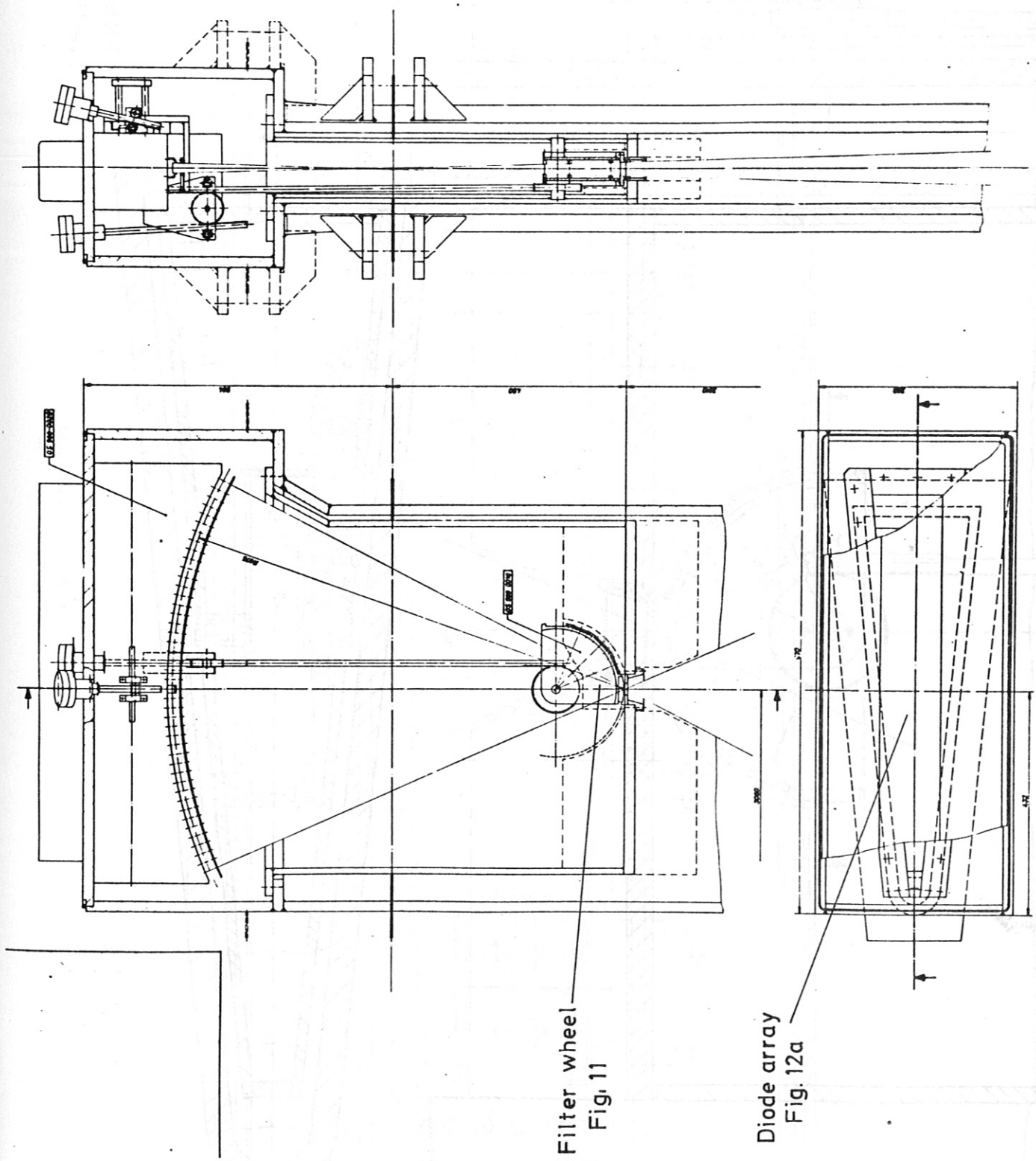

Fig. 10
Vertical camera

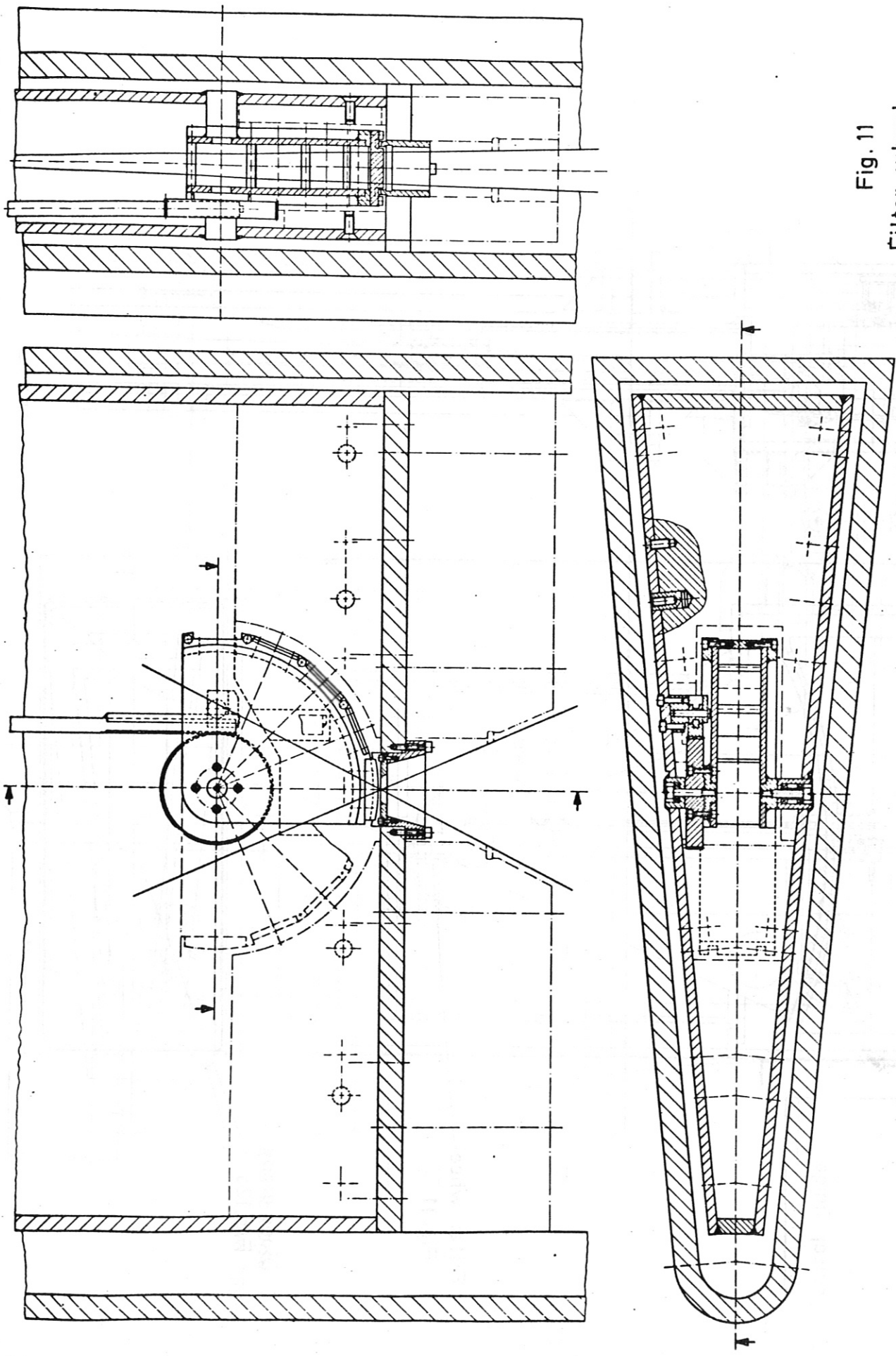

Fig. 11
Filter wheel
(vertical camera)

View from top

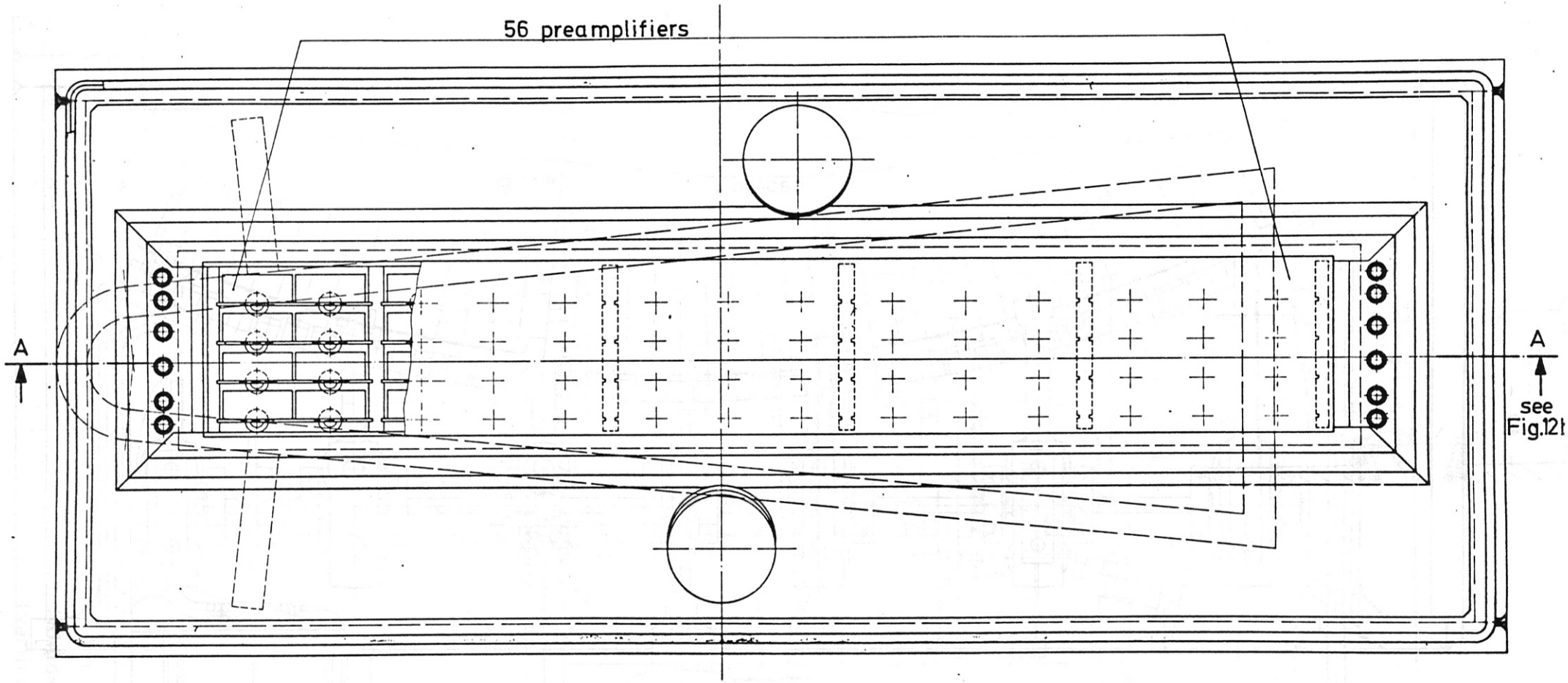

Fig. 12a
Diode array
(vertical camera)

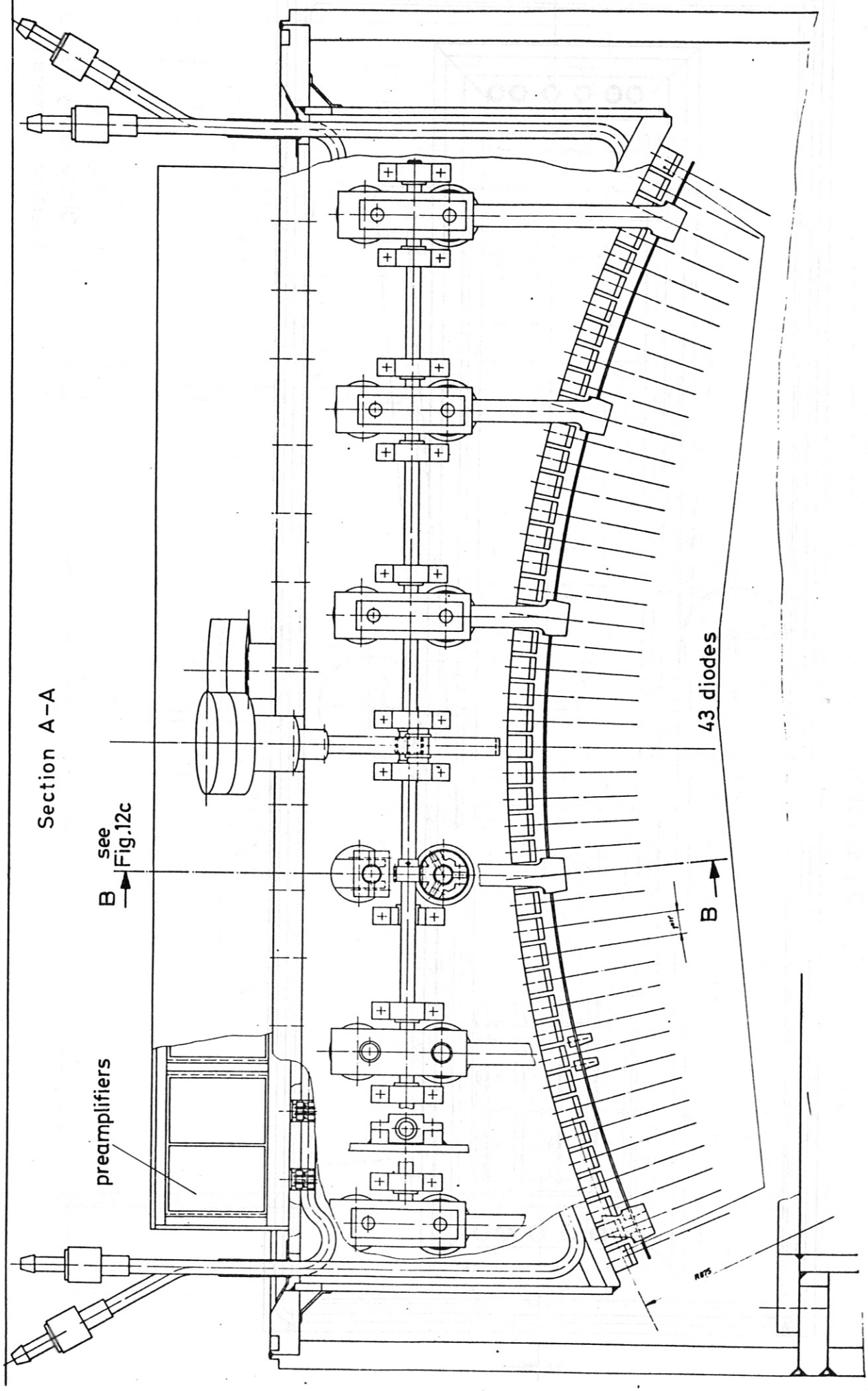

Fig. 12 b
Diode array
(vertical camera)

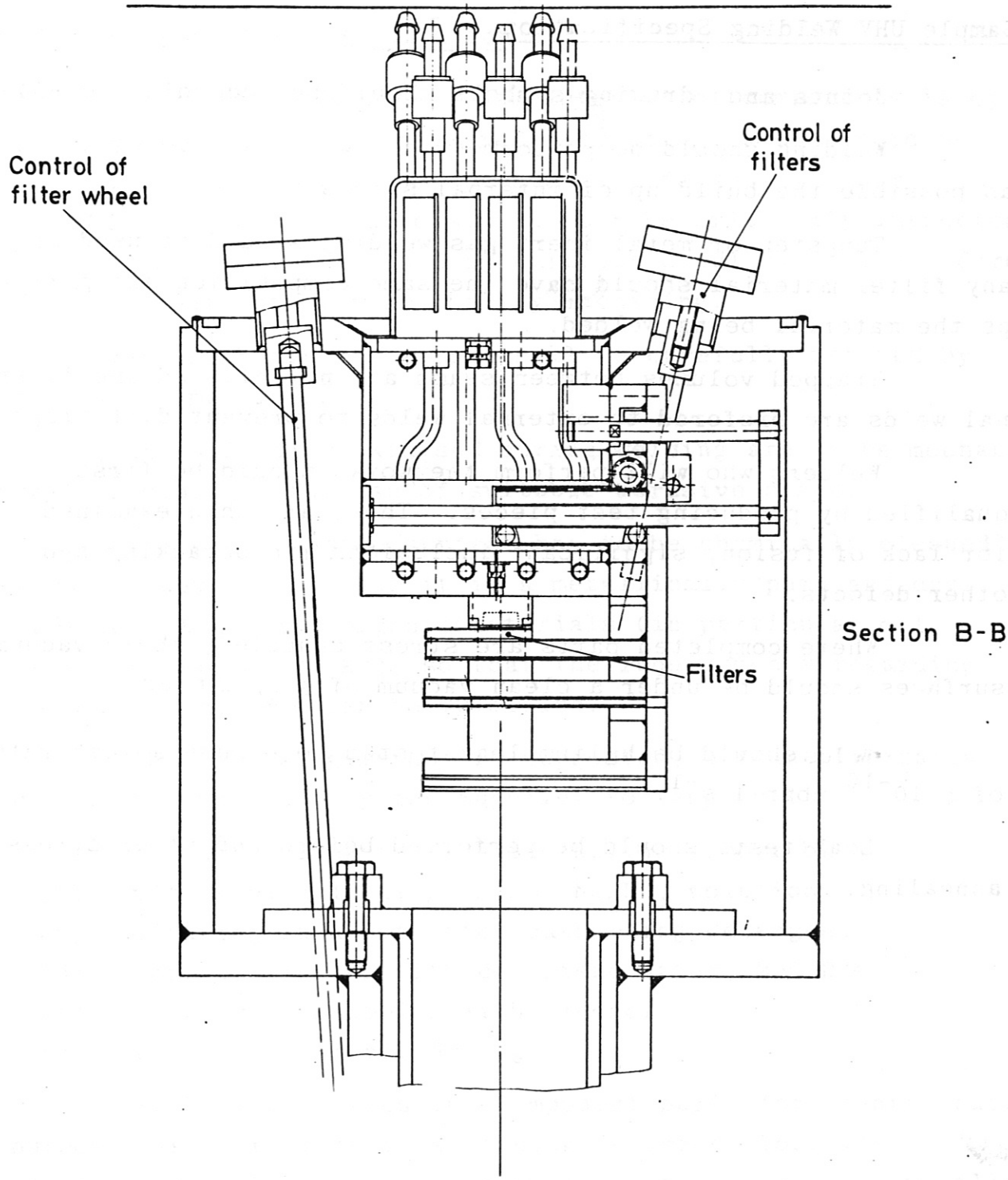

Fig. 12c
Diode array
(vertical camera)

Appendix A (JET Documentation)

Sample UHV Welding Specification

Joints and drawing symbols should be according to BS499

Welding should be performed in a way that avoids as far as possible the build up of internal stresses.

Tungsten or metal inert gas welding should be used and any filter material should have the same composition and purity as the material being welded.

Trapped volumes between seams are not allowed and internal welds are prefered to external welds to prevent dirt traps.

Welders who will perform the work, should be first qualified by producing test pieces. These are then examined for lack of fusion, significant inclusions, microcracking and other defects.

Where completed parts are stress annealed, their vacuum surfaces should be under a clean vacuum of $\lesssim 10^{-2}$ mbar.

Welds should be helium leak tested to ensure a leak rate of $\lesssim 10^{-10}$ mbar 1 s^{-1}.

Leak tests should be performed before and after stress annealing.

Appendix B (JET Documentation)

Sample UHV Cleaning Specification

The surface finish of the interior of components is of utmost importance if the required outgassing rates are to be achieved and the part is to operate satisfactorily under ultra-high vacuum conditions. It must be critically inspected for all imperfections caused by careless handling, sub-standard cleaning treatment or poor quality machining.

Any such imperfections shall be carefully removed by grinding or machining.

Areas locally oxidised during welding are to be mechanically cleaned by the use of suitable abrasive discs.

The whole inside surface has to be chemically cleaned in such a way as to leave it in a metallically pure and dry condition, free from organic materials (in particular oil, grease and finger marks), so that the requirements regarding the outgassing rate can be fulfilled.

The following method is suggested, but an alternative one may be submitted by the Supplier for approval:

(a) degrease using a trichlorethelyne vapour bath
(b) ultrasonic cleaning in hot Na_3PO_4 solution
(c) cleaning in a hot water bath using detergent
(d) copious rinsing with deionised water, 200 Ω/m
(e) rinsing or swabbing with alcohol
(f) dust free hot air drying

Marking of plates and component parts for identification purposes is to be done by embossing in agreed locations. Painting or marking with stamp or felt tip or tape is not allowed on any interior surface

APPENDIX 1

(JET DOCUMENTATION)

Class 1.

Routine or quasi routine operation. This would be required in normal operating conditions, with a relatively high frequency. Examples of typical machine operations which fall into this category are replacement of limiter plates and turbo-molecular pumps.

Class 2.

Emergency operations. These operations which would be necessary to get the machine back into working order when faults develop.

Remote handling requirements will influence the design to a reasonable extent, which is a trade off between the manufacturing cost and down time versus the designers estimation of the probability of a failure and the duration of the down time involved. Examples are replacement of bellows protection plates and vacuum leaks of the windows and window units.

Although in general repair and replacement of a diagnostic will not affect the basic operation of the machine and would therefore be defined in Class 3. Because this diagnostic forms part of the Torus vacuum system any vacuum faults would fall into Class 2, whilst Interferometer failures would fall into Class 3 which is defined below.

Class 3.

Replacement and repair operations on equipment which is not absolutely necessary for the running of the machine.

Special tools will be developed only when the need arises. Remote handling will be attempted, but the risk of failure is accepted.

Class 4.

No remote handling is involved.

5. Alternative Proposal for Shielding

Originally, a pure Inconel shielding was considered to be the only possible solution conforming to JET requirements. Although it was clear that such a shielding has relatively poor properties. Meanwhile we have found that for the DD phase of JET a combination of water, boron and Inconel (or partly stainless steel) constitutes a shielding which is much more effective and would certainly involve fewer problems as regards installing it in JET, and during operation.

The main advantage of the shielding containing water is the much higher attenuation of the neutrons. Detector tests in the Neuherberg nuclear reactor showed that the accuracy of the measurements in JET and the lifetime of the detectors will be limited by the neutron radiation. The concept of a pure Inconel shielding should therefore be abandoned.

The results of radiation transport calculations for DD plasmas are shown in Fig. 13. The curves give the ratio of the dose rates in silicon with and without a 200 mm thick shielding for different fractions of borated water and Inconel. Isotropic radiation and plane shielding geometry were assumed. This is an optimistic approximation but appears to be justified by the fact that a large fraction of neutron and γ-radiation will come from the torus structure, particularly the coils, where it is created or scattered.

From Fig. 13 we conclude that about 120 mm of the Inconel should be replaced by water. The γ-dose rate is then reduced another 1.4 times and the n-dose rate even 3.6 times. This choice of thickness ratio does not aim at the lowest possible total dose rate, but minimizes the effects due to neutron radiation, which are the most serious ones, and the mass and the heat capacity of the shielding. The detector dose rate in this configuration may be determined mainly by the radiation entering the camera through the aperture.

Figure 14 shows cross-sections of the shielding now proposed. The part inside the JET vacuum will be welded only onto the flange. It

consists essentially of a hollow Inconel container. Stainless steel plates, with a total thickness of ~70 mm are attached to the inner side of the rear wall. Either a ~2 mm thick boron-metal alloy can be put on their surface or 5 % boron acid has to be added to the water in order to absorbe the thermalized neutrons. During torus bake-out the water will be let out into an auxiliary container. CO_2 gas streaming through this volume could provide the heating and cooling in order to keep the shielding at the same temperature as the port. The mass of this part is then reduced from 2.5 tons to 1 ton (plus 200 kg water) and the necessary heating and cooling power from 12 KW to 4.5 KW. During JET pulses the shielding always has to be filled with water. A warning system has to be provided because attenuation without water is very low.

The design of the shielding outside the vacuum can be made much simpler; in particular, active heating and cooling does not appear to be necessary. Space is limited to about 100 mm; the highest possible attenuation will be achieved with lead covered with 25 to 50 mm of plastic material, e.g. polyethylene. Good thermal insulation between the lead (melting point 327° C) and camera walls will be provided by 10 mm Microtherm. Preferably the lead shielding is formed of several large blocks and installed after attachment of the camera. Removal is then possible any time.

As shielding at the rear polyethylene, also underlayed with Microtherm, is proposed. It has two advantages: The backscattering of neutrons is only 20 % compared with 80 % in the case of materials with higher Z, and it is very light. It can easily be removed during bake-out and for repair of, for example, the preamplifiers. Probably the rear shielding has to be mounted only for the last very intense DD pulses because the radiation coming back from the torus hall will be relatively weak.

The shielding outside the vacuum will reach a mass of 1 to 2 tons, the latter value being based on a lead thickness of 100 mm. A mass of 200 kg is represented by polyethylene.

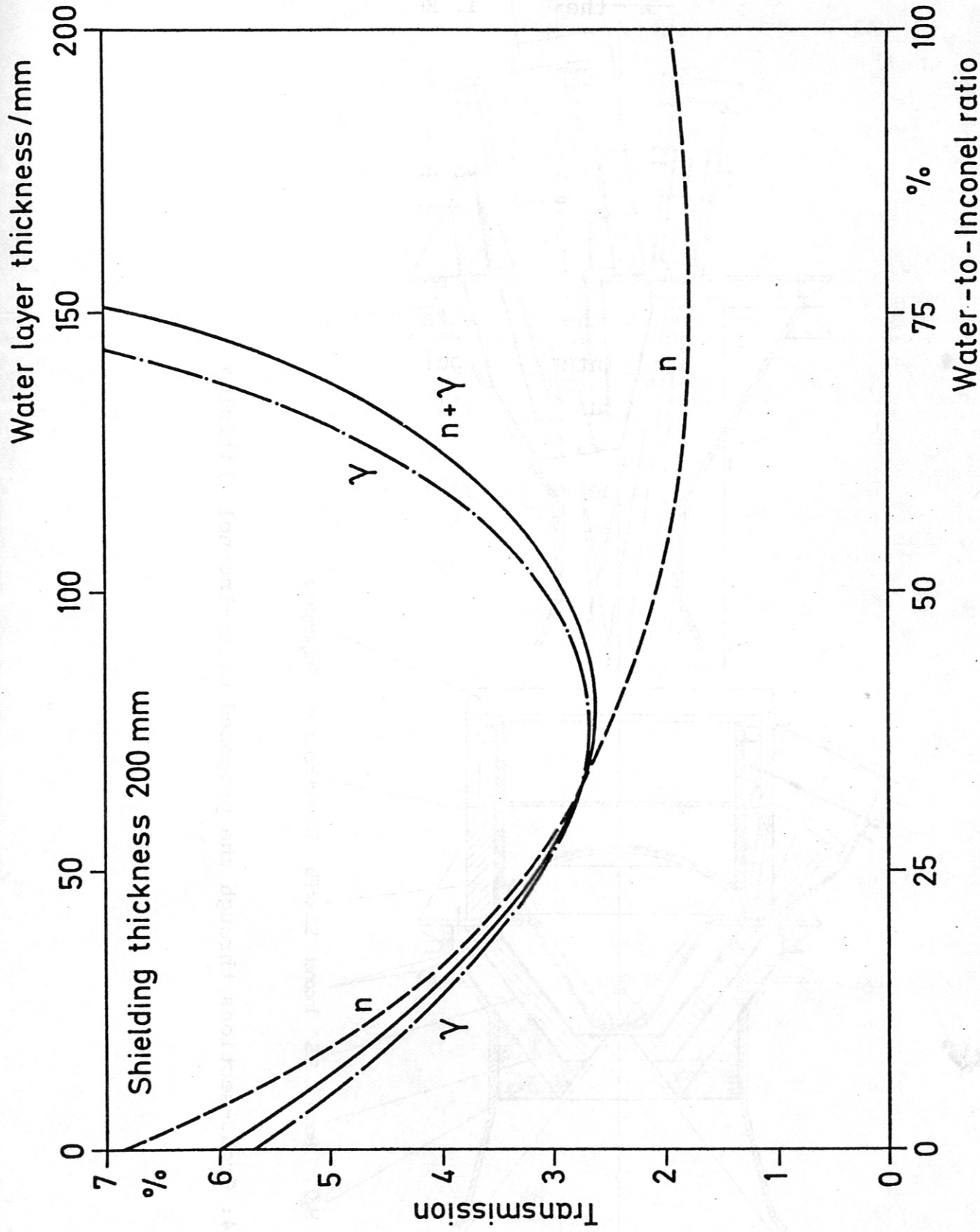

Fig.13: Calculated ratio of the neutron and gamma dose rates in the Si-diodes with and without shielding for different fractions of borated water and Inconel.

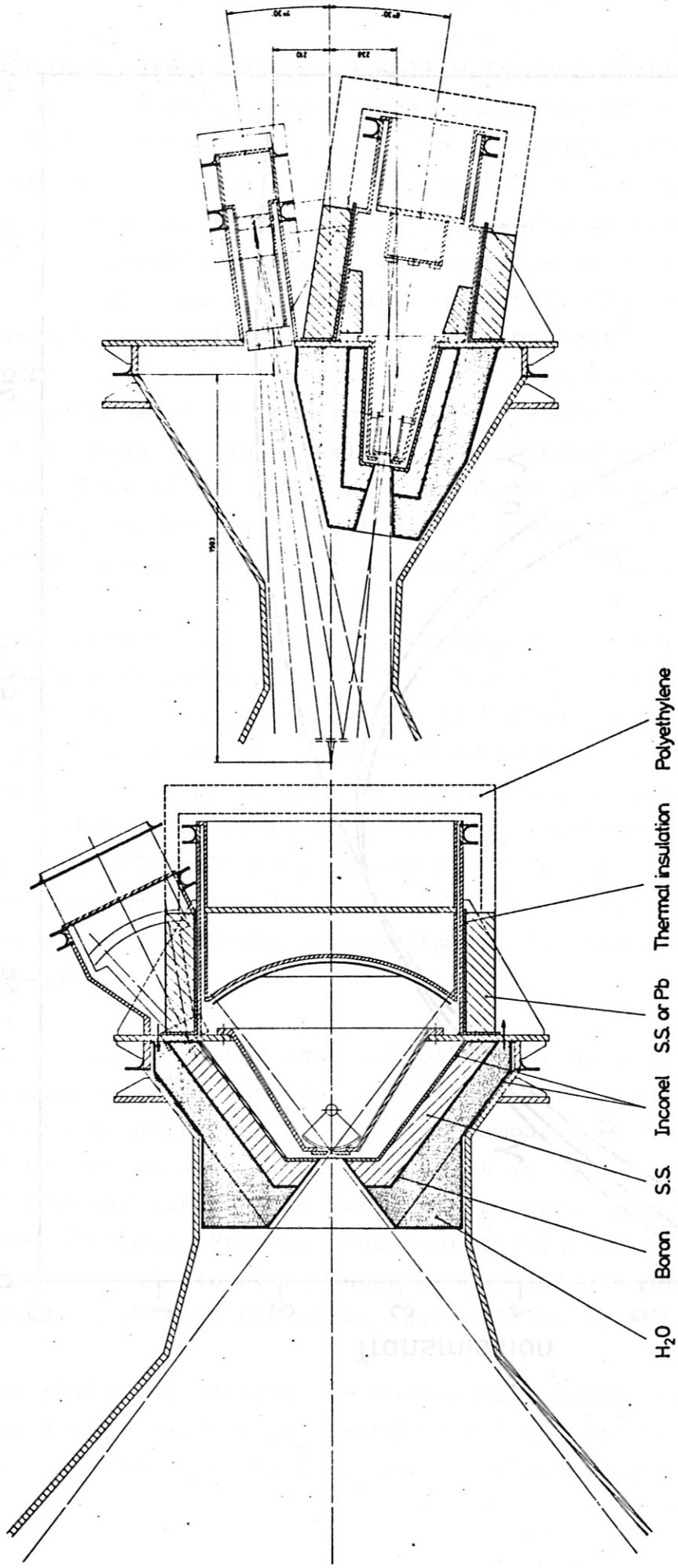

Fig. 14: Cross-sections through the proposed water-Inconel shielding